







International SCIENTIFIC WORKSHOP and POSTGRADUATE COURSE

Edited by:

Saša Haberl Meglič Damijan Miklavčič 2025

Organized by:





Supported by:























































November 10-15, 2025 Ljubljana, Slovenia

Proceedings of the



International SCIENTIFIC WORKSHOP and POSTGRADUATE COURSE

Edited by:

Saša Haberl Meglič Damijan Miklavčič

Organized by:	Supported by:
Organized by:	Supported by:

University of Ljubljana, **Bioelectrochemical Society**

Faculty of Electrical Engineering

International Society for Electroporation-Based

Institute of Oncology, Ljubljana Technologies and Treatments

Organising committee Abbott Ivy Biomedical Systems

Chair: ArgaMedtech Johnson&Johnson Medtech

Saša Haberl Meglič BIA Kardium

Boston scientific Kemomed

CardioFocus Members: Leroy Biotech

Carl Zeiss Lana Balentović, Klara Bulc-LifePulse Corp.

Rozman, Helena Cindrič, Duša **COBIK** Medtronic

Hodžić, Jernej Jurič, **ELEA** Mirai Medical

mPOR Samo Mahnič-Kalamiza, Urša Field Medical Primožič, Rok Šmerc, Zala Vidic **IGEA OMEGA**

Pulse Biosciences Imricor Medical Systems

> IonOptix Vitave

Iskra Medical

www.ebtt.org

Kataložni zapis o publikaciji (CIP) pripravili v Narodni in univerzitetni knjižnici v Ljubljani COBISS.SI-ID 255732739 ISBN 978-961-243-483-0 (PDF)

URL: https://2025.ebtt.org/

Copyright © 2025 Založba FE. All rights reserved. Razmnoževanje (tudi fotokopiranje) dela v celoti ali po delih brez predhodnega dovoljenja Založbe FE prepovedano.

Naslov: Proceedings of the Electroporation-based Technologies and Treatments

Založnik: Založba FE, Ljubljana

Izdajatelj: Fakuleta za elektrotehniko, Ljubljana Urednik: prof. dr. Sašo

Tomažič

Kraj in leto izida: Ljubljana, 2025

1. elektronska izdaja

Table of contents

Welcome note	5
INVITED LECTURERS AND NEW FACULTY MEMBERS	7
Helmut Puererfellner: My experience with the new pulsed field ablation (PFA) technology	9
Samo Mahnič-Kalamiza: The origin of bubbles in pulsed field ablation	10
Indrawati Oey: Pulsed electric fields for food processing applications	11
Antoni Ivorra: Collateral effects of electroporation: heating, electrical stimulation, and electrochemical reactions	13
Tobian Muir: Bleomycin electrosclerotherapy (BEST) in treatment of vascular malformations	14
Rafael V. Davalos: Irreversible electroporation as an ablation technique	15
Martijn Meijerink: The role of IRE in interventional radiology and oncology	16
Bostjan Markelc: Vascular effects in electroporation-based treatments	17
Frederic Deschamps: Electrochemotherapy in the management of spinal metastases	18
Quim Castellvi: Electrophysiological effects of electroporation on myocardium	19
Matevž Jan: Clinical experience with different pulsed field ablation systems for treatment of atrial fibrillation	20
SHORT PRESENTATIONS BY STUDENTS AND PARTICIPANTS	21
Nina Reitano-Ferber: Investigation of ion channel responses to nanosecond pulsed electric fields	23
Kateřina Červinková: Biochemiluminesce of PEF-induced protein oxidation under pro- and antioxidant conditions	24
Lana Balentović: Numerical modeling of unipolar intracardiac electrograms for assessing lesion transmurality after pu	
Nyah M. Ebanks: Computational model of the electric field distribution in a 3D tissue mimic	26
Argyrios Petras: Competing mechanisms for anisotropic lesion formation in cardiac PFA modelling	27
Simona Gelažunaitė: Assessing membrane permeabilization of Gram-negative bacteria using electrochemical impeda spectroscopy (EIS): differentiation from Gram-positive bacteria and evaluation of pulsed electric field (PEF) treatmen efficacy, with and without antibiotics	nt
Aimal Waheed: Electroporation-based transformation of Paenibacillus polymyxa: effects of voltage on pEGFP uptake kanamycin resistance	
Madita Kirchner: Non-uniformity of pulsed electric field treatment effects on plant tissues as evidenced by magnetic resonance imaging methods	
Aras Rafanavicius: Characterising H9c2 cell electroporation susceptibility in suspension and monolayer cultures	31
Kailee M. David: Advances in irreversible electroporation and elucidating cell death pathways	32

Maxime Berg: Impact of vascular lock on blood flow distribution under pulsed electric fields: experiments and simulations
James P. Villar-Mead: In vitro evaluation of pulsed field ablation-induced hemolysis using bovine blood in a benchtop model
Álvaro Borachok: Localized coronary vasospasm and flow velocity changes following pulsed field ablation
Maja Cvetanoska: Engineering of plasmids expressing bacterial toxins for in situ cancer vaccination
Eleni Zivla: Production and functional assessment of recombinant gelonin for electroporation applications
Bakhtawar Bibi: Assessing the safety of pulsed field ablation in the presence of implantable medical devices
Egle Mickeviciute-Zinkuviene: Strategies to mitigate bipolar cancellation in nano-electrochemotherapy for melanoma 39
Augustinas Želvys: High-power pulsed electromagnetic fields combination with calcium chloride or bleomycin for 4T1 breast cancer treatment: an <i>in vivo</i> study
Lara Snoj: Characterization of electrochemotherapy induced cell death pathways in vitro
Paulina Malakauskaite: Calcium electrochemotherapy using ultra-fast nanosecond electric pulses and their effects on mitochondria transmembrane potential and oxidation
Tanya Birk: Electrochemotherapy for spontaneous tumors in cats: establishing VetINSPECT platform43
Augustinas Šarkinas: Induction of the bystander effect in 3D cell cultures after electroporation-based treatments in vitro44
Diana Šiurnaitė: The investigation of synergistic effects of nivolumab and cisplatin electrotransfer in vivo

EBTT Proceedings 2025 Welcome note

Welcome note

Dear Colleagues, dear Participants, dear Students,

The Workshop and Postgraduate Course on Electroporation-Based Technologies and Treatments (EBTT) at the University of Ljubljana was organised for the first time in 2003. In more than twenty years, over 1100 participants from 45 different countries have attended the school. And also this year we can say with great pleasure: "with the participation of many of the world's leading experts in this field". However, the aims and objectives of the school remain unchanged: to provide participants with sufficient theoretical background knowledge and practical skills to enable them to use electroporation effectively in their working environment.

It is a great pleasure to welcome you to the EBTT organised by the University of Ljubljana and the Institute of Oncology Ljubljana, which takes place at the Faculty of Electrical Engineering as an integral part of the Interdisciplinary doctoral programme Biomedicine of the University of Ljubljana. From the very beginning, we were aiming to prepare lab work for the participants that would complement the lectures. Since the preparation of lab work takes more time than the preparation and organisation of lectures, we introduced lab work at the second workshop in 2005. The lab work covers different aspects of research: biological experiments in the cell culture labs, microbiology lab, tissue lab; numerical and molecular dynamics modelling, development of pulse generators and electrical measurements using the electronic lab workshop.

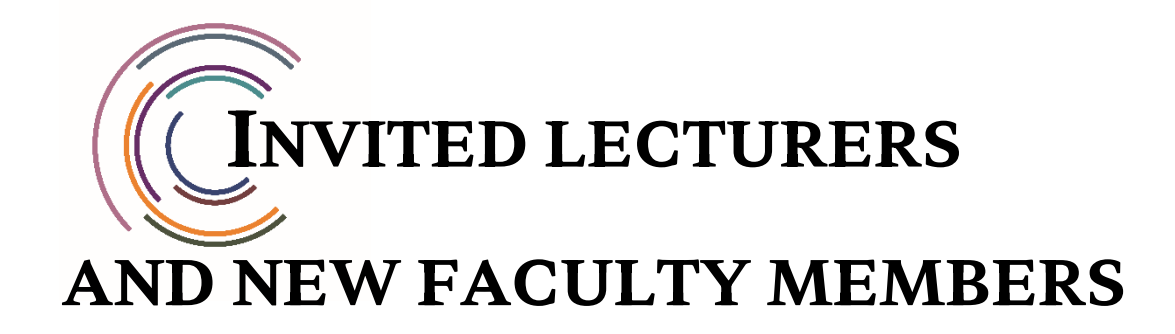
After the experience of 2020, when we organized the school completely online due to the pandemic, we decided to continue organizing the course as a hybrid course to enable participation even for those who still have difficulties with travel or suffer from a lack of time. The team here in Ljubljana will therefore offer both practical lab work on site and live webinars on the lab work so that you can benefit the most even if you are not in the lab. The biological experiments were pre-recorded and will be organized in the Infrastructural Centre "Cellular Electrical Engineering", part of the University of Ljubljana's network of research and infrastructure centres, in the Laboratory of Biocybernetics. Lab works would not be possible without the extensive participation and commitment of numerous members of the Laboratory of Biocybernetics, for which I would like to thank them all cordially.

It also needs to be emphasized that all written contributions included in the proceedings were thoroughly reviewed and subsequently edited. We would like to thank all authors and reviewers for their diligent work. I would also like to express our sincere gratitude to the faculty members and invited lecturers for their lectures delivered at the course. Finally, I would like to thank our sponsors as well as the Bioelectrochemical Society and the International Society for Electroporation-Based Technologies and Treatments for supporting us and making our EBTT possible.

I sincerely hope you will enjoy the experience, benefit from being with us and expand your professional network.

Sincerely Yours,

Damijan Miklavčič



My experience with the new pulsed field ablation (PFA) technology

Helmut Puererfellner; Ordensklinikum Linz Elisabethinen, Fadingerstraße 1, 4020 Linz, AUSTRIA

INTRODUCTION

This tutorial-oriented lecture provides a comprehensive overview of Pulsed Field Ablation (PFA) in the treatment of atrial fibrillation (AF). The tutorial value of this lecture lies in its structured approach to explaining PFA, covering initial expectations, real-world experiences, workflow integration, and future outlook.

UNDERSTANDING PFA AND ITS MODALITIES

The lecture introduces different PFA catheter designs, including circular, pentaspline, focal, largetip, and balloon-based systems [1], [2], [3]. In addition, the technical considerations for optimal lesion sets, circumferential pulmonary vein isolation (PVI), and posterior wall isolation are discussed [4].

CLINICAL EFFICACY AND SAFETY

Insights from pivotal clinical trials, such as the PULSED AF trial [5] and the inspIRE trial [6] demonstrate the safety, efficiency, and durability of PFA compared to traditional radiofrequency (RF) and cryoablation techniques [7]. Success rates, tissue selectivity, and lesion durability are evaluated using remaps at 3 and 12 months, emphasizing the potential of PFA to become the preferred technology for *de novo* PVI [6], [8].

PRACTICAL CONSIDERATIONS

The lecture shares hands-on experiences with PFA, highlighting a short learning curve but also challenges such as sheath and spline management, air ingress, and stroke risk [9]. Comparisons between PFA and conventional thermal ablation reveal key takeaways, including the potential for false impressions of safety regarding PV narrowing and the need for integrating 3D mapping systems for improved lesion durability [6], [10].

FUTURE DIRECTIONS AND THE "HYPE CYCLE" OF PFA

While single shot PFA is regarded as a safe, efficient, and operator-independent technique, its long-term efficacy, lesion durability, and head-to-head comparisons with traditional ablation modalities remain areas of active investigation [8], [11]. The lecture discusses next steps in PFA technology evolution, including 3D electro-anatomical mapping (EAM) integration, second-generation devices, and dosing optimization [3], [6].

CONCLUSIONS

This lecture provides a valuable roadmap for electrophysiologists looking to integrate PFA into clinical practice. It offers a balanced perspective on its advantages, limitations, and ongoing research, reinforcing that while the hype around PFA is justified, further studies are needed to refine its applications and confirm long-term outcomes.

- [1] Chen S., *et al.* 2025 International expert practical guide on the use of the pentaspline pulsed field ablation system in atrial fibrillation ablation procedures. *Circ Arrhythm Electrophysiol*, 18(8), 2025.
- [2] Tilz R.R., *et al.* Safety and effectiveness of the first balloon-in-basket pulsed field ablation system for the treatment of atrial fibrillation: VOLT CE Mark Study 6-month results. *Europace*, 27:euaf072, 2025.
- [3] De Potter T., *et al.* Dual energy for pulmonary vein isolation using focal ablation technology integrated with a three-dimensional mapping system: SmartfIRE 12-month results. *Europace*, 27:euaf174, 2025.
- [4] Pürerfellner H., *et al.* Controversy: the blanking period after atrial fibrillation ablation is needed and should be maintained. *Europace*, 1:euaf203, 2025.
- [5] Verma A., *et al.* Pulsed field ablation for the treatment of atrial fibrillation: Pulsed AF pivotal trial. *Circulation*, 147:1422-1432, 2023.
- [6] De Potter T., *et al.* Predictors of success for pulmonary vein isolation with pulsed-field ablation using a variable-loop catheter with 3D mapping integration: complete 12-month outcomes from inspIRE. *Circ Arrhythm Electrophysiol*, 17, 2024.
- [7] Boersma L., et al. Progress in atrial fibrillation ablation during 25 years of *Europace* journal. *Europace*, 25:euad244, 2023.
- [8] Ekanem E., *et al.* Safety of pulsed field ablation in more than 17,000 patients with atrial fibrillation in the MANIFEST-17K study. *Nat Med*, 30:2020-2029, 2024.
- [9] Tilz R. R., *et al.* A worldwide survey on incidence, management, and prognosis of oesophageal fistula formation following atrial fibrillation catheter ablation: the POTTER-AF study," *EHJ*, 44:2458-2469, 2023.
- [10] Duytschaever M., et al. Dual energy for pulmonary vein isolation using dual-energy focal ablation technology integrated with a three-dimensional mapping system: SmartfIRE 3-month results. Europace:26:euae088, 2024.
- [11] De Potter T. J. R., *et al.* Long-term clinical benefits of pulsed field ablation in paroxysmal atrial fibrillation: subanalyses from the multicenter inspIRE trial. *Circ Arrhythm Electrophysiol*, 18 (5), 2025.

The origin of bubbles in pulsed field ablation

Samo Mahnič-Kalamiza¹, Damijan Miklavčič¹, Peter Lombergar¹, Blaž Mikuž², Lars M. Mattison³, Daniel C. Sigg³, Bor Kos¹; ¹University of Ljubljana, Faculty of Electrical Engineering, Ljubljana, SLOVENIA; ²Jožef Stefan Institute, Reactor Engineering Division, Ljubljana, SLOVENIA; ³Medtronic, Mounds View, MN, USA

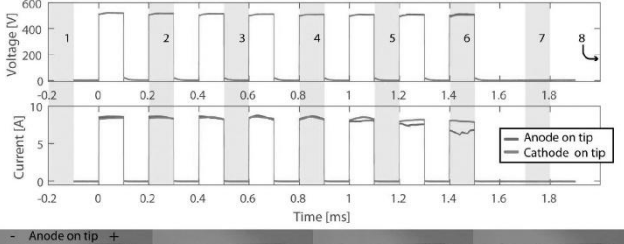
INTRODUCTION

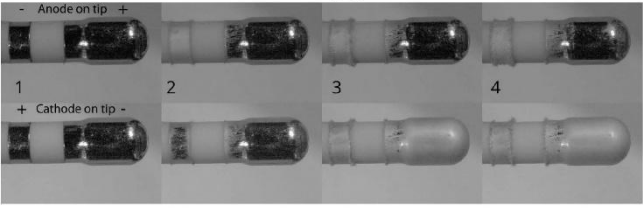
Bubble formation during pulsed field ablation (PFA) raises concerns about embolic risk. Three main mechanisms of their origin are proposed: boiling [1,5], electrolysis [2,3], and degassing [3,4]. Distinguishing between them is essential to improve safety and optimize ablation protocols.

MATERIALS AND METHODS

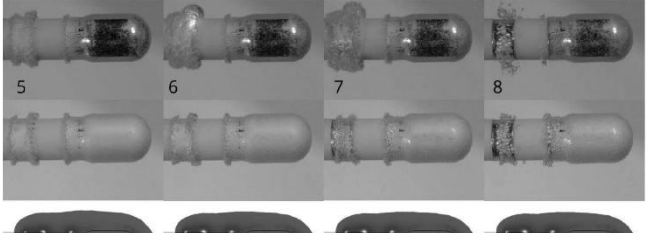
Experiments were performed in saline using a modified RF ablation catheter. Monophasic and biphasic pulse protocols were delivered, while bubble dynamics were recorded with a 10,000 fps high-speed camera. Numerical simulations of electric and thermal fields were performed in COMSOL Multiphysics to identify hotspots.

RESULTS AND DISCUSSION









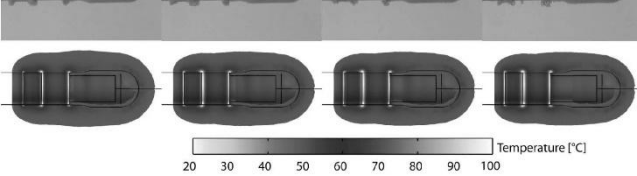


Figure 1: Delivery of monophasic (100 μ s, 5 kHz, n = 8, train duration 1.5 ms) pulses between the catheter tip and ring electrodes – high-speed camera images and numerical simulations of heating.

High-speed imaging showed that monophasic pulses produced stable, persistent bubbles consistent

with electrolysis, whereas biphasic pulses generated transient vapor bubbles that quickly collapsed.

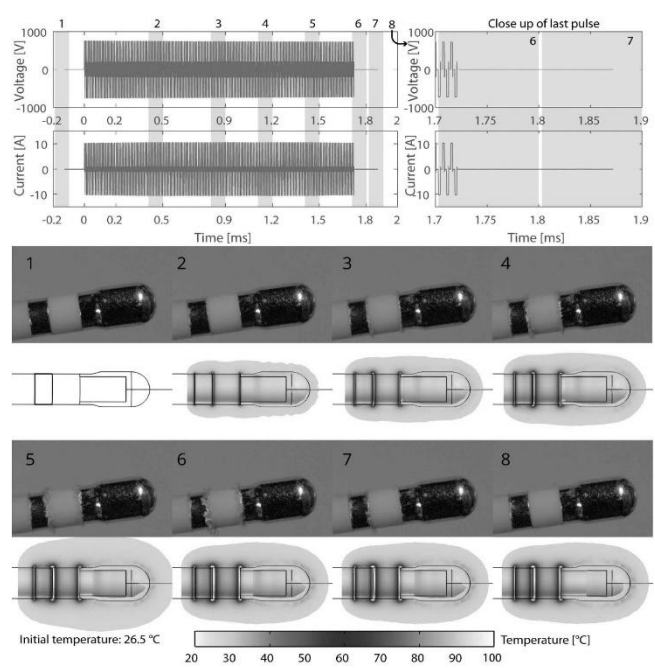


Figure 2: Delivery of biphasic pulses $(2-2-2-2 \mu s, n=216, train duration 1.73 ms) imaged by the high-speed camera, with corresponding numerical simulations of heating.$

Modelling confirmed hotspots near electrode edges coinciding with boiling onset, while electrolysis-driven bubbles originated from and persisted due to electrode reactions. Degassing, though contributing a smaller gas volume than boiling or electrolysis, can still generate long-lived bubbles, which may persist in the bloodstream.

CONCLUSIONS

Electrolysis dominates bubble formation in monophasic PFA, while biphasic pulses primarily induce transient boiling. Protocols with short biphasic pulses and optimized geometry minimize bubble generation and improve safety.

- [1] Verma A., et al., Pulsed field ablation for atrial fibrillation: PULSED AF pivotal trial results. Circ Arrhythm Electrophysiol, 14, 2021.
- [2] Aycock K.N., *et al.*, Irreversible electroporation: background, theory, and review of recent developments in clinical oncology. *Bioelectricity*, 1:214-234, 2019.
- [3] van Es R., *et al.*, In vitro analysis of the origin and characteristics of gaseous microemboli during catheter electroporation ablation. *J Cardiovasc Electrophysiol*, 30:2071-2079, 2019.

Pulsed electric fields for food processing applications

Indrawati Oey^{1,2}, Sze Ying Leong^{1,2}; ¹Department of Food Science, University of Otago, PO BOX 56, Dunedin 9054, NEW ZEALAND; ²Riddet Institute, Palmerston North, NEW ZEALAND

Pulsed Electric Field (PEF) technology applies short, repetitive, high-voltage pulses across food placed between two electrodes. This technology has emerged as a versatile tool in food processing, extending beyond traditional pasteurization and extraction to functional food design through facilitating modulation of food macromolecules via microstructural and molecular alterations. The core mechanisms underpinning PEF effects include electroporation/pore formation, electrochemical reactions and Joule heating, which collectively modify cellular and macromolecular structures to influence food quality and nutritional outcomes.

MICROBIAL INACTIVATION & PRESERVATION

PEF combined with preheating has been commercially used as a low-temperature alternative to thermal pasteurization, particularly in fruit juices [1], where it effectively inactivates vegetative microorganisms but not spores, while preserving color, flavor, and nutrients of the juice products. Process validation protocols with surrogate microorganisms to simulate PEF pasteurization conditions have been proposed for dairy milk [2] as well as the emerging high-protein plant-based milk alternatives [3].

EXTRACTION AND YIELD ENHANCEMENT

By disrupting cell structures, PEF facilitates enhanced mass transfer processes involving extraction of sugars, pigments, juices, and bioactive compounds. This capability has been exploited in juice, olive oil, and wine production to improve yields and reduce processing times [4]. In Merlot and Pinot Noir grapes, PEF pretreatment shorten the cold maceration process while increasing anthocyanin extraction and improve antioxidant protection in human cell models [5,6].

PEF pretreatment also accelerates moisture diffusion, reducing drying times in fruits, vegetables and meat matrices, which improves energy efficiency and quality of the final dried products [7].

STRUCTURE MODIFICATION OF PLANT FOODS

The most prominent food industrial application of PEF is in the potato and tuber sectors, where it modifies plant tissue structure to smooth surfaces, reduce surface sugars, enhance texture, improve cutting quality, accelerate blanching time by up to 50%, ensure consistency in color upon deep frying, and decrease frying oil uptake [4]. PEF enhances yield and sensory attributes of vegetable chips, improving crunchiness which influences satiation responses in consumers [8]. PEF also modulate the texture of legumes which affects human chewing behaviour and improves nutrient digestibility [9].

INNOVATION ON MEAT PROCESSING

PEF is applied on tough and low-value meat cuts to improve their tenderization, increase brine absorption (reducing tumbling time by up to 50%), enhance water-holding capacity, and support aging. Notably, a semi-continuous PEF chamber capable of processing

10 kg of meat in seconds has recently been developed. New breakthrough application on sous-vide bone-in beef short ribs further show improvements in cooking quality, color, and tenderness with the help of a PEF pre-treatment [10].

MODIFICATION OF STARCH AND PROTEIN DIGESTIBILITY

PEF could modify digestibility of starch-rich food matrices by disrupting granule structure and crystallinity. At moderate energy inputs, PEF reduces their rapidly digestible starch (RDS) and increases resistant starch (RS) by approximately 48%, slowing glucose release during simulated gastrointestinal digestion. At higher energy inputs, RDS however increases, accelerating digestion. These changes are linked to disruption of amylose-lipid complexes and altered gelatinization behavior [11]. Regarding protein digestibility, PEF at mild to moderate intensities shows tendency to unfold tertiary and quaternary structures exposing enzymatic sites, potentially increasing digestibility. Excessive PEF energy may cause protein aggregation, reducing digestibility. PEF can also inactivate anti-nutritional enzymes like trypsin inhibitors, enhancing protein utilization [12]. Such findings have been observed across soy, pea, and dairy proteins.

MODIFICATION OF RHEOLOGY PROPERTIES

PEF also effectively produces chickpea gels with varying textures. Gels produced by PEF showed an increase in RDS and faster intestinal protein digestion rates during digestion, indicating improved nutrient bioaccessibility and tailored textures. PEF has recently been found to change the viscosity of dairy milk proteins. Moreover, using PEF as pasteurisation step before fermentation alters the rheology and starch and protein digestibility of plant-based yoghurts [12].

PEF AS GERMINATION ABIOTIC STRESSOR

PEF pretreatment enhances germination efficiency of legumes and seeds as well as bioprotective capacity and nutrient digestibility, e.g. PEF at 0.5 kV/cm improved starch and protein digestibility, especially for 72 h germinated cereal seeds. The combined PEF and germination treatment offers a promising strategy to enhance the nutritional profile of seeds, catering to health-conscious consumers [13, 14].

PEF technology offers a multifaceted approach to food processing, enabling microbial safety, enhanced extraction, accelerated drying, and tailored structural modifications. Critically, its ability to modulate starch and protein digestibility through controlled microstructural and molecular changes opens avenues for designing functional foods with targeted nutritional profiles. The integration of PEF in novel food design, highlights its potential in personalized nutrition and sustainable food innovation.

- [1] Kantala C., *et al.* Evaluation of pulsed electric field and conventional thermal processing for microbial inactivation in Thai orange juice. *Foods*, 11:1102, 2022.
- [2] Sharma P., et al. Microbiological and enzymatic activity of bovine whole milk treated by pulsed electric fields. Int J Dairy Technol, 71:10-19, 2018.
- [3] Horlacher N., *et al.* Effect of pulsed electric field processing on microbial and enzyme inactivation in blended plant-based milk alternatives: A case study on a microbial challenge test for a non- presterilized oat-based beverage enriched with pea protein. *IFSET*, 94:103699, 2024
- [4] Lee, P.Y., *et al.* Prospects of pulsed electric fields technology in food preservation and processing applications from sensory and consumer perspectives. *IFSET*, 59:6925-6943, 2024.
- [5] Leong S. Y. *et al.* Evaluation of the anthocyanin release and health-promoting properties of Pinot Noir grape juices after pulsed electric fields. *Food Chem*, 196:833-841, 2016.
- [6] Leong, S. Y. et al. Effect of combining pulsed electric fields with maceration time on Merlot grapes in protecting Caco-2 cells from oxidative stress. Food Bioprocess Technol, 9:147-160, 2016.
- [7] Lammerskitten A., *et al.* Pulsed electric field pretreatment improves microstructure and crunchiness of freeze-dried plant materials: Case of strawberry. *LWT*, 134: 110266, 2020.

- [8] Cahayadi J., et al. Textural effects on perceived satiation and ad libitum intake of potato chips in males and females. Foods, 9:85, 2020.
- [9] Alpos M., *et al.* Influence of pulsed electric fields (PEF) with calcium addition on the texture profile of cooked black beans (*Phaseolus vulgaris*) and their particle breakdown during in vivo oral processing. *IFSET*, 75:102892, 2022.
- [10] Karki R., *et al.* Effect of chilled storage on the quality, invitro protein digestibility, and microbial growth of sous vide processed beef short ribs pre-treated with pulsed electric field (PEF). *IFSET*, 89:103485, 2023.
- [11] Alpos M., *et al.* Understanding in vivo mastication behaviour and in vitro starch and protein digestibility of pulsed electric field-treated black beans after cooking. *Foods*, 10:2540, 2021.
- [12] Horlacher N., *et al.* Synergistic effects of PEF treatment and lactic acid fermentation on protein digestibility and texture in a blended oat and pea yogurt alternative. *LWT*, 220:117587, 2025.
- [13] Leong S. Y., *et al.* Electropriming of wheatgrass seeds using pulsed electric fields enhances antioxidant metabolism and the bioprotective capacity of wheatgrass shoots. *Sci Rep*, 6:25306, 2016.
- [14] Johnston C., et al. Low-intensity pulsed electric field processing prior to germination improves in vitro digestibility of faba bean (Vicia faba L.) flour and its derived products: A case study on legume-enriched wheat bread. Food Chem, 449:139321, 2024.

Collateral effects of electroporation: heating, electrical stimulation, and electrochemical reactions

Antoni Ivorra; Department of Engineering, Universitat Pompeu Fabra, Carrer Roc Boronat 138, 08018 Barcelona, SPAIN

INTRODUCTION

Applying electrical energy to living tissues for inducing electroporation can cause diverse phenomena in addition to electroporation. Three well-identified collateral phenomena, which in most cases are undesired, are heating, electrical stimulation, and electrochemical reactions.

HEATING

Except for superconductors, all electrical conductors dissipate electrical energy in the form of heat when current flows through them. This phenomenon is known as Joule heating or resistive or Ohmic heating and obeys:

$$P = I^2 R$$

where P is the power of heating, I is the current flowing through the conductor and R is its resistance. This equation, known as Joule's law, can also be expressed for infinitesimal volumes at each point of space:

$$p = \frac{\left|\vec{J}\right|^2}{\sigma} = \left|\vec{E}\right|^2 \sigma$$

 $p=\frac{{|\vec{J}|}^2}{\sigma}={|\vec{E}\,|}^2\sigma$ where σ is the electrical conductivity and \vec{I} and \vec{E} are the current density and electric field respectively. In electroporation scenarios, with field magnitudes in the order of hundreds of V/cm and conductivities in the order of S/m, Joule heating would cause harmful temperatures if very short exposures, much shorter than a second, were not used. The dependence of heating on the square of the electric field is relevant because it implies that heating is particularly high where the electric field is larger, typically at the periphery of the electrodes due to the edge effect. This is further exacerbated by the increase of σ with the temperature.

The temperature increase due to the Joule effect can be accurately predicted with numerical models, even for complex tissues. However, thermal damage models used to predict the physiological impact of the intense temperature peaks caused during electroporation are intended for longer exposures and, although are used by the electroporation community, their accuracy is still unknown.

ELECTRICAL STIMULATION

The nervous system transmits signals in the form of action potentials. Action potentials are sudden transitions in transmembrane resting voltage that propagate along the cell. Electrical stimulation consists in nonphysiologically triggering action potentials by delivering electric fields.

In clinical applications of electroporation, electrical stimulation is not desired because, by exciting efferent nerves, it causes muscle contractions and, by exiting afferent nerves, it causes pain [1].

Both electroporation and electrical stimulation occur when the transmembrane voltage is artificially increased above a threshold due to the presence of the electric field. This implies that unsought stimulation occurs very frequently when electroporation is intended. Advantageously, highfrequency biphasic fields can cause electroporation whilst minimizing electrical stimulation [2].

ELECTROCHEMICAL REACTIONS

Electrical conduction in metallic electric circuits is provided by the flow of electrons whereas in living tissues (and in suspensions) the moving charge carriers are ions. Conduction across the interface between the electronic conductor and the ionic conductor, that is, across the electrode, can be capacitive or electrochemical. Capacitive conduction is only substantial for very brief or ac currents of small magnitude. In most electroporation scenarios, conduction across the electrode is mediated by electrochemical reactions. In electrochemical reactions, the chemical species in the living tissue and the electrode exchange electrons thus altering their chemistry.

reactions Electrochemical generally are deleterious for electroporation applications because they modify pH and cause the release of gases and metallic ions. (However, it is worth noting that it has been proposed their synergy with electroporation to achieve large ablation volumes [3]).

Electrochemical reactions are a surface phenomenon (occur at the electrode) and, because of that, are of particular concern when the electrode area is large compared to the treated volume, as is typically the case in microfluidic setups.

Electrochemical reactions are difficult to model, particularly at the anode (positive electrode) because multiple reactions can occur concurrently.

Interestingly, high-frequency biphasic currents minimize electrochemical reactions. This effect, combined with lower stimulation, explains the emergence of high-frequency biphasic fields for electroporation-based ablation.

- [1] Cvetkoska A., et al. Muscle contractions and pain sensation accompanying high-frequency electroporation pulses. Sci Rep, 12:8019, 2022.
- [2] Mercadal B., et al. Avoiding nerve stimulation in irreversible electroporation: a numerical modeling study. Phys Med Biol, 62:8060-8079, 2017.
- [3] Klein N., et al. Single exponential decay waveform; a synergistic combination of electroporation and electrolysis (E2) for tissue ablation. PeerJ, 5:e3190,

Bleomycin electrosclerotherapy (BEST) in treatment of vascular malformations

Tobian Muir; James Cook University Hospital, Marton Road, Middlesbrough, TS43BW, UNITED KINGDOM

INTRODUCTION

Bleomycin injection is an effective treatment of vascular malformations with low adverse event rates [1]. Multiple repeat treatments are however needed to achieve a response. The application of a novel technology solution by the addition of electroporation has shown significant promise in a variety of clinical assessments.

METHODS

Bleomycin is a large, hydrophilic, charged molecule and is very poorly permeable to all cell membranes [2].] A novel method of applying an electric field to cells, delivered by a handheld needle electrode, overcomes the poor cell permeability and allows for enhanced transfer of Bleomycin into cells. This technique is called electroporation. The addition of electroporation to Bleomycin increases the cellular uptake and cytotoxicity by up to 700 times. [3]. This has been successfully used in cancer treatment in the technique of electrochemotherapy. Electrochemotherapy is a safe and effective treatment with minimal morbidity. [4]. The proof of concept in applying the same technology to vascular malformations was provided by a pilot trial: Electrosclerotherapy as a Novel Treatment Option for Hypertrophic Capillary Malformations [5].

RESULTS

Following the publication of a significant response achieved in a vascular malformation in clinical practice after a single bleomycin electrosclerotherapy treatment in 2017 [6], the publication of a number of retrospective [7] and prospective [8] case series followed, including a retrospective, multi-centre case series on 233 patients [9]. These show a decrease of 86% in the size and a complete response in 57% of treatment resistant malformations. appearance following BEST were improved in 55% and perfect in 10% with low complication rates. A current NIHR multi-centre trial is ongoing assessing the patient reported outcomes in adults and children undergoing BEST treatment of vascular malformations [10]. To support the learning curve and standardising care, a Current Operating Procedure (COP) has recently been published [11].

CONCLUSIONS

Although in an early stage, the enhanced treatment results with the addition of electroporation in BEST is

exciting and very promising for patients presenting with this challenging disease.

Further research is needed to fully understand the immunological and molecular mechanisms involved and to improve and enhance clinical results.

- [1] Horbach S. E., *et al.*, Intralesional bleomycin injections for vascular malformations: a systematic review and metaanalysis. *Plast Reconstr Surg*, 137: 244-256, 2016.
- [2] Gothelf A., *et al.* Electrochemotherapy: results of cancer treatment using enhanced delivery of bleomycin by electroporation. *Cancer Treat Rev*, 29:371-378, 2003.
- [3] Orlowski S., *et al.* Transient electropermeabilization of cells in culture. Increase of the cytotoxicity of anticancer drugs. *Biochem Pharmacol*, 37:4727-4733, 1988.
- [4] Miklavcic D., *et al.* Electrochemotherapy: from the drawing board into medical practice. *Biomed Eng Online*, 13: 29, 2014.
- [5] Horbach S., et al. Electrosclerotherapy as a novel treatment option for hypertrophic capillary malformations: A randomized controlled pilot trial. Dermatol Surg, 46:491-498, 2020.
- [6] McMorrow L., et al. Bleomycin electrosclerotherapy: new treatment to manage vascular malformations. Br J Oral Maxillofac Surg, 55:977-979, 2017.
- [7] Wolgemuth W., et al. Bleomycin electrosclerotherapy in therapy-resistant venous malformations of the body. J Vasc Surg Venous Lymphat Disord, 3:731-739, 2021.
- [8] Kostusiak M., *et al.* Bleomycin electrosclerotherapy treatment in the management of vascular malformations. *Dermatol Surg*, 48:67-71, 2022.
- [9] Schmidt V. F., *et al.* Outcome of bleomycin electrosclerotherapy of slow-flow malformations in adults and children. *European Radiology*, 34:731-6425-6434, 2024.
- [10] ClinicalTrials.gov ID NCT05494710/ IRAS 248206 Bleomycin Electrosclerotherapy Treatment of Vascular Malformations: A Feasibility Study (BEST)
- [11] Muir T., *et al.* Current operating procedure (COP) for bleomycin ElectroScleroTherapy (BEST) of low-flow vascular malformations. *Radiol Oncol*, 58:469-479, 2024.

Irreversible electroporation as an ablation technique

Rafael V. Davalos; Department of Biomedical Engineering, Georgia Tech, Atlanta, GA 30318, USA

INTRODUCTION

Irreversible Electroporation (IRE) is a minimally invasive tissue ablation technique that involves applying low-energy pulses to create nanoscale defects in the lipid bilayer, inducing cell death. [1]. High frequency irreversible electroporation (H-FIRE) [2], otherwise known as biphasic Pulsed Field Ablation (PFA), is a next-generation form of IRE and is being used for the treatment of cardiac arrhythmias, cancer, and other malignancies. This new therapy mitigates the need for intraoperative paralytics to prevent involuntary pulse-related muscle contractions. IRE and H-FIRE are unique among ablation techniques, as they only affect the cell membrane while tissue molecules such as collagen structures and proteins remain intact, thereby making treatment near previously inoperable critical structures possible. Further, they facilitate a robust immune response by releasing damage-associated molecular pathways (DAMPs) and disease-specific antigens in their native state [3].

By modifying the pulse parameters and field strength, the ablation can be tuned to specific modes of cell death [5] to produce non-inflammatory (e.g., apoptosis) or pro-inflammatory (e.g., necrosis, pyroptosis, and necroptosis) responses [3,4]. We will discuss these mechanisms and their effect on the innate and adaptive immunological response.

We will also discuss numerical modeling techniques to accurately predict the field distributions and corresponding ablation volumes within the tissue as a function of these waveforms. In addition to modeling the field distribution, we will discuss how to accurately model the temperature distribution as a function of various pulse parameters, which is crucial for mitigating thermal damage in many of these applications.

Finally, this lecture will cover recent advances in pulsed electric field therapies to target other aspects of the tumor microenvironment and potential clinical applications.

- [1] Davalos R. V., *et al.* Tissue ablation with irreversible electroporation. *Ann Biomed Eng*, 33:223-231, 2005.
- [2] Arena C.B., *et al.* Theoretical considerations of tissue electroporation with high-frequency bipolar pulses. *IEEE Trans Biomed Eng*, 58, 2011.
- [3] Ringel-Scaia V.M., *et al.* High-frequency irreversible electroporation is an effective tumor ablation strategy that induces immunologic cell death and promotes systemic anti-tumor immunity. *EBioMedicine*, 44, 2019.
- [4] Mercadal B., *et al.* Dynamics of cell death after conventional IRE and HFIRE treatments. *Ann Biomed Eng*, 48, 2020.
- [5] Polajzer T., *et al.* Immunogenic cell death in electroporation-based therapies depends on pulse waveform characteristics. *Vaccines*, 11, 2023.

The role of IRE in interventional radiology and oncology

 $\label{lem:martin} \textit{Martijn Meijerink}; \textit{Department of Radiology \& Nuclear Medicine Amsterdam University Medical Centers (Amsterdam UMC), Amsterdam, THE NETHERLANDS}$

NOTES

Vascular effects in electroporation-based treatments

Bostjan Markelc^{1,2}; ¹Department of Experimental Oncology, Institute of Oncology Ljubljana, SLOVENIA; ²Department of Biology, Biotechnical Faculty, University of Ljubljana, SLOVENIA

INTRODUCTION

Electroporation/electropermeabilization (EP), i.e. the application of electric pulses to cells or tissue, leads suitable conditions to a reversible permeabilization of the cell membranes and thus facilitates the entry of exogenous molecules into the cells. Reversible EP of tissue is feasible, efficient and tolerable in humans. The most advanced routine clinical application is electrochemotherapy (ECT), in which cytotoxic drugs are delivered to cells to treat tumors. More recently, this approach has also been used in the treatment of vascular malformations, termed where it has been bleomycin electrosclerotherapy (BEST). If excess electric pulses are applied, this leads to irreversible electroporation (IRE). The use of IRE to treat various types of cancer is intensively researched and several clinical trials are ongoing. In addition, IRE has recently been successfully adapted for the treatment of cardiac arrhythmias, where it is referred to as pulsed field ablation (PFA). Since the early experiments with EP and ECT in mouse tumors, it became clear that the EPbased treatments have an effect on the normal and tumor vasculature in addition to the direct cytotoxic effect of the therapy on the tumor cells. This is now directly exploited in BEST and is also recognized as adverse event in the treatment of cardiac arrhythmias.

RESPONSE OF ENDOTHELIAL CELLS TO ELECTROPORATION

Endothelial cells, which form the inner lining of blood vessels, exhibit varying sensitivity to EP depending on electric field intensity, pulse duration, and tissue type. In vitro studies on human endothelial cells have shown that reversible EP induces cytoskeletal changes, most notably disruption of actin and tubulin filaments, followed by disruption of cell-tocell junctions, which control vascular permeability [1]. Moreover, in vitro studies demonstrated that EP increases the permeability of endothelial monolayers in a dose-dependent manner.

DIFFERENTIAL EFFECTS OF EP AND ECT ON NORMAL AND TUMOR BLOOD VESSELS

The application of EP pulses to normal blood vessels increases the permeability of the affected blood vessels, causes transient vascular lock, i.e. a decrease in perfusion, and modulates the diameter of the affected blood vessels. Similarly, the application of EP or ECT to tumors increases the permeability of the affected blood vessels and causes vascular lock [2]. In normal blood vessels, these effects are short-lived,

whereas in tumor vessels they are long-lasting and persist more than 72 hours after ECT.

In tumors, EP leads to an immediate abrogation of blood flow, i.e. a vascular lock that lasts for more than 60 min. Interestingly, the tumor-supplying arterioles react to EP in the same way as normal vessels, namely with rapid vasoconstriction and increased permeability [3]. This suggests that this is the main cause of the immediate vascular lock observed after EP. EP also leads to increased permeability of tumor blood vessels to macromolecules and a partial, long-lasting decrease in perfusion. Thus, EP has a differential effect on normal and tumor blood vessels. Moreover, ECT has a direct cytotoxic effect on tumor endothelial cells, i.e. it has a vascular disrupting effect, which is now also exploited in BEST.

EFFECTS OF IRE ON BLOOD VESSELS

The effects of IRE on blood vessels were first confirmed with magnetic resonance imaging (MRI) of perfusion in the rat brain after EP, showing that IRE increases the permeability of blood vessels to macromolecules [4]. Importantly, further studies conducted on various normal blood vessels showed that while IRE can destroy the endothelial cells, the large blood vessels retain their functionality and are repopulated with endothelial cells after therapy.

CONCLUSIONS

In summary, EP-based treatments have effects on the endothelial cells and thus on the normal and tumor vasculature. This can be exploited to destroy endothelial cells, as is the case with ECT and BEST, or one can rely on their function-preserving property when it comes to normal blood vessels, as is the case with IRE and PFA.

- [1] Kanthou C., *et al.* The endothelial cytoskeleton as a target of electroporation-based therapies. *Mol Cancer Ther*, 5:3145-52, 2006.
- [2] Jarm T., *et al.* Antivascular effects of electrochemotherapy: implications in treatment of bleeding metastases. *Expert Rev Anticancer Ther*, 10:729-46, 2010.
- [3] Markelc B., *et al.* Differential mechanisms associated with vascular disrupting action of electrochemotherapy: intravital microscopy on the level of single normal and tumor blood vessels, *PLoS One*, 8: e59557, 2013.
- [4] Hjouj M., *et al.* MRI study on reversible and irreversible electroporation induced blood brain barrier disruption. *PLoS One*, 7: e4281, 2012.

Electrochemotherapy in the management of spinal metastases

Frederic Deschamps; *Interventional radiology department, Institute Gustave Roussy, Villejuif, FRANCE*

INTRODUCTION

Electrochemotherapy (ECT) is a minimally invasive therapy that can be used for the locoregional treatment of spinal metastasis. ECT refers to the concomitant application of reversible electroporation intravenous administration of bleomycin, with electroporation enhancing bleomycin uptake into the cells. Electroporation is a phenomenon that occurs when cells are exposed to short and intense electric pulses that induce changes in the transmembrane potential difference. Electroporation requires the insertion of electrodes in or around the tumour, and subsequently high-intensity electric pulses are delivered to cause cellular membrane damages. Depending on electric pulses amplitude and number of pulses applied, electroporation can be reversible, with membrane permeability recovery and cell survival, or irreversible, with loss of cell homeostasis and cell death, termed irreversible electroporation (IRE) [1].

The purpose of electroporation is to facilitate the passage of non-permeant molecules into the cell cytoplasm. Bleomycin is the molecule used for ECT because of its capacity to induce mitotic cells death. Indeed, bleomycin is binding to DNA and producing single and double strand breaks by the formation of an activated oxygen complex and is selectively toxic to cells in the M and G2 phases of the cell cycle, and generally more effective against actively dividing rather than resting cells.

RESULTS

Hence, while IRE may not be ideal for vertebral metastases due to concerns for permanent spinal cord injury, the chemotherapeutic damage caused by reversible electroporation may provide a novel and unique treatment opportunity. Thus, a recent retrospective study [2] has demonstrated that ECT can rescue radiotherapy-resistant epidural spinal cord compression (Fig.1,2) in 40 metastatic cancer patients, providing rapid and durable pain relief and

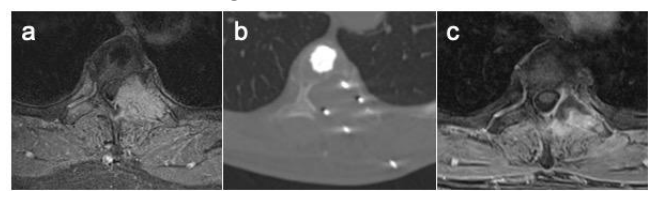


Figure 1: Large thyroid metastasis with epidural extension (a). Electrochemotherapy (b) resulted in complete necrosis at 1 month (c).

neurological improvement.

At 1 month, pain was significantly improved over baseline (median Numerical Rating Score: 1.0 [0-8] versus 7.0 [1.0-10], P < .001) and neurological

benefits were considered as marked (28%), moderate (28%), stable (38%), or worse (8%). In addition, 1-month post-treatment MRI (35 patients) demonstrated complete response in 46% of patients, partial response in 31%, stable disease in 23%, and no patients with progressive disease.

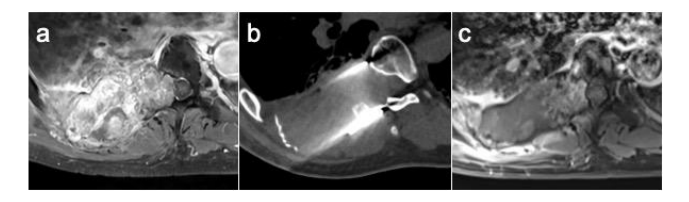


Figure 2: Kidney metastasis compressing with epidural extension (a). Electrochemotherapy (b) resulted in decompressing the spinal cord at 1 month (c).

CONCLUSIONS

Based on very promising tumour response rate in bone metastases [3] and particularly in vertebral metastases [2], ECT is becoming a new percutaneous option in the therapeutic arsenal of interventional oncology. It offers an alternative when thermalablation techniques are contraindicated and will probably compete palliative radiotherapy in the near future.

However, despite theoretical safety profile, 7.5% of paraplegia and 10% of nerve toxicity have been reported in the literature [2] after ECT of spinal metastasis with epidural extension. This toxicity is related to the inevitable inhomogeneity of the electric field between electrodes, with unexpected hyperthermia and IRE at the vicinity of the electrodes' tips.

To enhance ECT's clinical applicability in the treatment of spinal metastases, further numerical and preclinical studies are required to determine the optimal parameters that create an electric field below the IRE threshold across the spinal cord and over the reversible electroporation threshold across tumour.

- [1] Mir L. M., et al. Mechanisms of electrochemotherapy. Adv Drug Deliv Rev, 35:107-118, 1999.
- [2] Deschamps F., *et al.* Electrochemotherapy in radiotherapy-resistant epidural spinal cord compression in metastatic cancer patients. *Eur J Cancer*, 186:62-68, 2023.
- [3] Campanacci L., *et al.* Electrochemotherapy is effective in the treatment of bone metastases. *Curr Oncol*, 29:1672-1682, 2022.

Electrophysiological effects of electroporation on myocardium

Quim Castellvi^{1,2}; ¹Department of Information and Communication Technologies, Universitat Pompeu Fabra, E-08018 Barcelona, SPAIN; ²Cardiofocus, Marlborough, Massachusetts 01752, USA

INTRODUCTION

Pulsed Field Ablation (PFA) is an increasingly consolidated modality for cardiac ablation that offers a potentially safer and shorter procedure times compared to traditional thermal ablation methods [1]. In PFA, electric pulses are commonly delivered using an endoluminal catheter which induces irreversible electroporation (IRE) to the myocardium surrounding the electrode location. While the tissue under IRE results in a durable ablative lesion, reversible electroporation (RE) beyond the that area can induce a transient electrophysiologic signal disruption [2].

Intracardiac electrograms (iEGMs) have traditionally been used to assess the formation of cardiac lesions. However, PFA's stunning effect can lead to overestimation of the treated area, potentially compromising treatment efficacy.

To improve the success rates of PFA treatments, a deeper understanding of the electrophysiological effects of electroporation is essential. This knowledge will support the development of novel intra-procedural measurements to predict lesion durability.

This lecture will provide an overview of the primary electrophysiological effects of electroporation on the myocardium and discuss current approaches for evaluating the irreversibility of PFA-induced lesions.

ELECTROPHYISIOLOGIC EFFECTS

The sudden membrane conductivity increase induced by electroporation triggers initially the depolarization of cardiomyocytes as excitable cells. However, during the resealing process, the interactions between the induced ion leaks, membrane channels, and the altered transmembrane voltage prevent the normal depolarization of the cell.

Although, in-vitro studies [3] and numerical models have been employed to elucidate this complex mechanisms, further studies are still needed to fully understand the electrophysiological response to electroporation.

Despite the current lack of knowledge, several methods have been already proposed to be used as feedback methods to guide the physicians during the procedures.

INTRACARDIAC ELECTROGRAMS

Conventional bipolar iEGMs are obtained by measuring the potential difference between two electrodes placed around the region of interest. While this approach offers high spatial resolution of the cardiac surface, it lacks information about deeper

myocardial layers. Unipolar iEGMs, recorded between a single electrode at the area of interest and a dispersive electrode, have been shown to contain information correlated to lesion extension and durability.

TISSUE ELECTRIC PROPERTIES

Impedance measurements have been widely adopted by the electrophysiology community as an indicator of lesion formation in thermal ablations. This passive electrical properties of the tissue, already proposed as a potential tool for real-time monitoring in electroporation procedures [4], could be able of discriminating between reversible and irreversible areas in the myocardium.

TISSUE OPTICAL PROPERTIES

Optical Coherence Reflectometry (OCR) is a non-invasive imaging technique with microscopic resolution. When combined with a Polarization-Sensitive system (PS-OCR), tissue birefringence can be measured. This optical property correlates with tissue microstructural anisotropy which is high in healthy myocardium. When exposed to irreversible damage, the affected tissue loses its ultrastructure, resulting in a reduction in birefringence [5]. Since myocytes with reversible effects preserve their ultrastructural conformation, PS-OCR can be used as a feedback mechanism.

- [1] Ekanem E., *et al.*, Safety of pulsed field ablation in more than 17,000 patients with atrial fibrillation in the MANIFEST-17K study. *Nat Med*, 30:2020-2029, 2024.
- [2] Verma A., et al. Primer on pulsed electrical field ablation: understanding the benefits and limitations. Circ Arrhythmia Electrophysiol, 902-917, 2021.
- [3] Chaigne S., *et al.* Reversible and irreversible effects of electroporation on contractility and calcium homeostasis in isolated cardiac ventricular myocytes. *Circ Arrhythmia Electrophysiol*, 15:E011131, 2022.
- [4] Castellví Q., et al. Assessment of electroporation by electrical impedance methods. in *Handbook of Electroporation*, 99, pp. 671–690, *Cham: Springer International Publishing*, 2017.
- [5] Terricabras M., et al. Cardiac pulsed field ablation lesion durability assessed by polarization-sensitive optical coherence reflectometry. Circ Arrhythmia Electrophysiol, 17:E012255, 2024.

Clinical experience with different pulsed field ablation systems for treatment of atrial fibrillation

Matevž Jan¹, Andrej Pernat², Tine Prolič Kalinšek¹, Jernej Štublar¹, Jernej Iršič¹; ¹Department for Cardiovascular Surgery; ²Department for Cardiology, University Medical Centre Ljubljana, Liubljana, SLOVENIA

INTRODUCTION

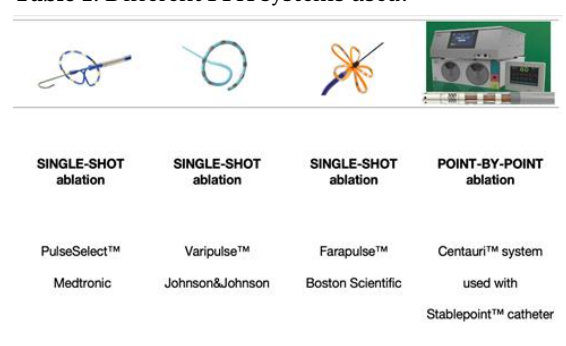
Pulsed field ablation (PFA) as a nonthermal ablation method is increasingly used in clinical practice for treatment of atrial fibrillation (AF) [1]. Several studies have shown favorable procedural parameters and safety profile with similar efficacy when compared to the traditional thermal methods of ablation [2]. We present our experiences with different PFA systems.

METHODS

This is a single center retrospective analysis. Consecutive patients referred to our hospital for treatment of atrial fibrillation were included. Four PFA systems were used (Table 1). Pulmonary vein isolation (PVI) was the endpoint of all procedures, with posterior left atrial wall isolation (PWI) only in selected patients. The choice of the system was at the discretion of the operating physician. Additionally, some patients with persistent atrial fibrillation were included in a randomized trial (Electro AF, NCT06134752) comparing effectiveness of point-by-point PFA with radiofrequency ablation (RFA). We evaluated procedural parameters, adverse events, acute procedural outcome in the majority of included patients. In patients included in the randomized trial we also evaluated long term ablation lesion (PVI and PWI) durability with reassessment procedures.

All procedures were performed either in deep sedation or general anesthesia. Activated clotting time was kept at 300-350s, 1 mg of Atropine was administered prior to the start of ablation in the majority of patients. Procedural time, left atrial dwell time, acute procedural success and possible adverse events were recorded. Major adverse events were defined as those requiring immediate medical intervention and those resulting in prolonged hospital stay or long term disability.

Table 1: Different PFA systems used.



RESULTS

One hundred and thirty-nine patients were treated, 58 with a point-by-point PFA, 81 with a single-shot PFA. Demographic characteristics are shown in Table

2. Procedural data and adverse events are shown in Table 3. Acute procedural success - isolation of pulmonary veins (PVI) and posterior left atrial wall (PWI) where applicable – were reached in all patients (100%). There were no major adverse events.

In patients included in the randomized trial reassessment procedures revealed similar rate of PVI in PFA and RFA (per patient 75 vs 66%, NS; per vein 83 vs 83%) and higher rate of PWI in PFA compared to RFA (PFA 92 vs RFA 17%, p= 0.001).

Table 2: Demographic characteristics. BMI, body mass index; LAVI, left atrial volume index; LVEF, left ventricular ejection fraction.

Number of patients	r of patients 139		
Age (average years ± SD)	62 ± 9		
Gender	83 % male, 17 % female		
BMI (average ± SD)	29 ± 5		
Type of AF	27 % persistent, 73 % paroxysmal		
LAVI (average ml/m ² ± SD)	46 ± 12		
LVEF (average % ± SD)	57 ± 13		

Table 3: Procedural data and adverse events per PFA system. LA, left atrium.

PFA system used	PulseSelect™	Varipulse™	Farapulse™	Centauri™ system
Number of patients	35	15	31	58; 48% persistent AF
Lesion type (PVI, PWI)	PVI in all, PWI in 4	PVI in all	PVI in all, PWI in 4	PVI and PWI in persistent AF
Procedural time average minutes ± SD)	101 ± 23	82 ± 28	82 ± 18	165 ± 42
LA dwell time average minutes ± SD)	72 ± 15	67 ± 26	65 ± 21	153 ± 44
Acute success - PVI and PWI	100%	100%	100%	100%
Adverse events	0	1 device failure	1 severe vagal reaction, 1 device failure	1 severe vagal reaction, 2 severe coughing

CONCLUSIONS

Our clinical experience shows that PFA is a safe and acutely effective treatment of AF.

Point-by-point PFA results in a higher rate of durable PWI in comparison to RFA.

- [1] Chun K.-R. J., *et al.* State-of-the-art pulsed field ablation for cardiac arrhythmias: ongoing evolution and future perspective. *Europace*, 26:euae134, 2024.
- [2] Htay P. N., *et al.* Pulsed field ablation: a systematic review. *Health Sci Rep*, 8:e70439, 2025.



Investigation of ion channel responses to nanosecond pulsed electric fields

Nina Reitano-Ferber¹, Nina Van¹, Patricia Nabos¹, Florence Poulletier De Gannes¹, Isabelle Lagroye^{1,2}, Philippe Leveque³, Delia Arnaud-Cormos³, Noëlle Lewis¹, Rosa Orlacchio^{1,2} and Yann Percherancier¹; ¹Univ. Bordeaux, CNRS, Bordeaux INP, IMS, UMR 5218, F-33400 Talence, FRANCE; ²Ecole Pratique des Hautes Etudes, PSL Research University, 75014 Paris, FRANCE; ³Univ. Limoges, CNRS, XLIM, UMR 7252 F-87000 Limoges, FRANCE

INTRODUCTION

Recent studies suggest that nanosecond pulsed electric fields (nsPEF) may influence ion channel behavior by inducing conformational changes. While several reports have highlighted the ability of nsPEFs to affect cellular activity [1,2], the underlying mechanisms, particularly whether they involve direct modulation of channel gating or indirect effects such as membrane permeabilization, remain under debate.

In this context, ion channels are of particular interest due to their central roles in processes such as pain perception, excitability, and cell signaling. Clarifying how nsPEFs interact with these proteins could open new perspectives for bioelectrical control strategies.

Our project aims to experimentally explore the impact of nsPEF on ion channels using genetically encoded Bioluminescence Resonance Energy Transfer (BRET)-based biosensors [3], which enable non-invasive, real-time monitoring of molecular events in living cells.

METHODS

To monitor ion channel behavior in real time, we generated BRET-based biosensors by fusing donor and acceptor pairs (mNeonGreen/nLuc or rGFP/rLuc) to selected ion channels of interest, including members of the TRP, VGIC, and TREK families. These biosensors allow dynamic tracking of conformational changes or calcium fluxes at the plasma membrane or in intracellular compartments.

Constructs were transiently transfected in HEK293T cells cultured either as monolayers (2D) or spheroids (3D). Sensor functionality was first validated using chemical stimulation.

In parallel, a dedicated platform is currently under development to synchronize nsPEF delivery with BRET signal acquisition. The system includes a delivery system and a fiber-coupled spectrometer for live-cell photon detection.

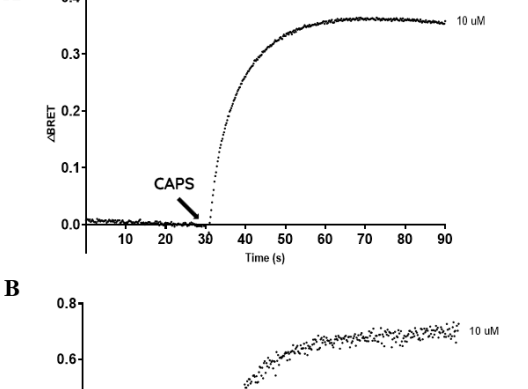
RESULTS AND FIGURES

To validate our genetically encoded BRET biosensors, we monitored the activation of TRPV1 channels upon stimulation with Capsaicin (CAPS) in HEK293T cells. The $\Delta BRET$ signal was recorded in real time using two distinct cell formats: standard 2D monolayers and 3D spheroid cultures.

In 2D cells, the addition of CAPS triggered a rapid and sustained increase in the BRET signal, indicating conformational changes consistent with TRPV1 activation (Figure 1A). In 3D spheroids, the biosensors also responded robustly to CAPS, with a preserved kinetic profile despite the increased tissue-like complexity (Figure 1B).

These results confirm that our BRET probes are sensitive and functional across different cell

architectures, establishing a reliable foundation for future nsPEF exposure experiments.



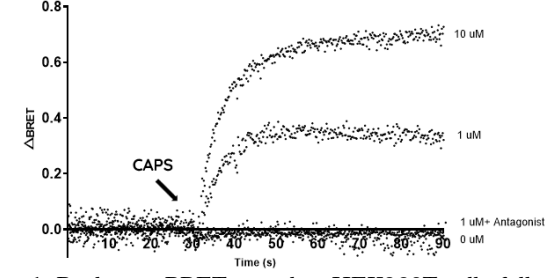


Figure 1: Real-time BRET signal in HEK293T cells following chemical stimulation with Capsaicin. (A) Monolayer (2D) cells show rapid increase in Δ BRET signal post-injection. (B) Spheroids (3D) maintain a measurable BRET response post-injection.

CONCLUSION

With validated biosensors and an operational nsPEF delivery platform, our study provides a solid basis to explore how ion channels respond in live cells. This will allow us to test whether certain pulse parameters can lead to observable changes in their activity.

- [1] Burke R., et al. Nanosecond pulsed electric fields depolarize transmembrane potential via voltage-gated K⁺, Ca²⁺ and TRPM8 channels in U87 glioblastoma cells. Biochim Biophys Acta Biomembr, 1859:2040-2050, 2017.
- [2] Yang L., *et al.* Nanosecond electric pulses differentially affect inward and outward currents in patch clamped adrenal chromaffin cells. *PLOS ONE*, 12:e0181002, 2017.
- [3] Chappe Y., *et al.* Genetically-encoded BRET probes shed light on ligand bias-induced variable ion selectivity in TRPV1 and P2X5/7. *Proc Natl Acad Sci USA*, 119: e2205207119, 2022.

Biochemiluminesce of PEF-induced protein oxidation under pro- and antioxidant conditions

Kateřina Červinková¹, Petra Vahalová¹, Daniel Havelka¹, Viliam Kolivoška², Michal Cifra¹; ¹Institute of Photonics and Electronics of the Czech Academy of Sciences, 18200 Prague, CZECHIA; ²J. Heyrovský Institute of Physical Chemistry of the Czech Academy of Sciences, 18200 Prague, CZECHIA

INTRODUCTION

Biochemiluminescence is weak but detectable light emitted when biomolecules react with reactive oxygen species (ROS). Pulsed electric fields (PEF) are widely used in biomedicine and food processing, yet their oxidative effects on proteins remain incompletely defined. Here, we use biochemiluminescence to track PEF-driven ROS formation and quantify how pro- and antioxidant agents reshape the emission signal before, during, and after pulsing, yielding new insight into PEF-induced oxidative processes in proteins [1].

METHODOLOGY

We built a parallel-plate PEF chamber (2 mm gap; steel anode and perforated steel cathode) coupled to a photomultiplier. Bovine serum albumin (BSA, 0.6 mM) and a conductivity-matched phosphate buffer control were exposed to 30 unipolar pulses (1470 V,

BSA far beyond buffer controls, indicating synergy between Fenton-type chemistry (via albumin-bound metals) and interfacial ROS generation. Antioxidants modulated these dynamics: CAT reduced signals by consuming $\rm H_2O_2$; SOD lowered signals most prominently during pulsing, implicating involvement of superoxide in PEF.

CONCLUSION

Time-resolved biochemiluminescence provides a label-free, in-situ readout of PEF-driven oxidative chemistry in protein solutions and cleanly resolves how pro- and antioxidants act across pre-, during-, and post-pulsing windows. These findings establish biochemiluminescence as a practical monitor for optimizing PEF protocols and additive chemistries in protein-containing media.

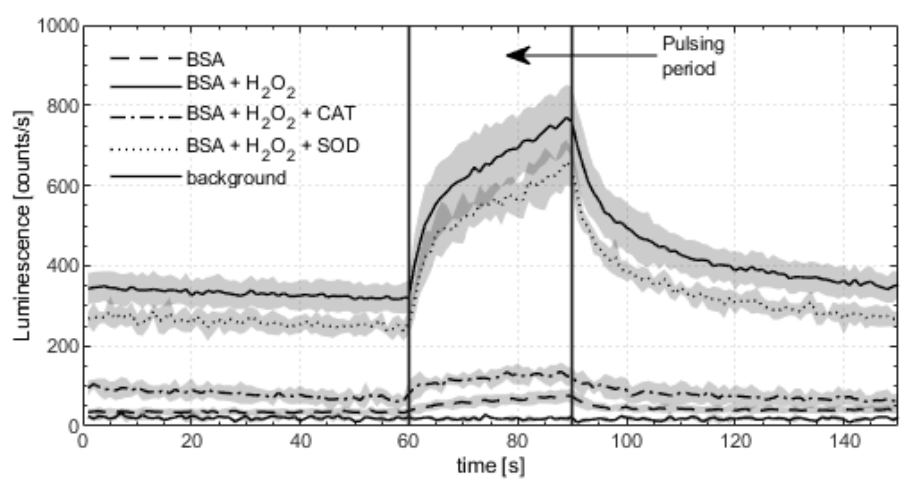


Figure 1: Averaged luminescence transients obtained in PEF experiments performed with BSA in the absence and presence of H_2O_2 and with additionally introduced antioxidant enzymes (CAT or SOD).

100 $\mu s,~1$ Hz; field $\approx~0.735~MV~m^{-1}).$ (Bio)chemiluminescence was recorded in three time windows: pre-pulsing (0–60 s), pulsing (60–90 s), and post-pulsing (90–150 s). Pro-oxidant $H_2O_2~(1~mM)$ and antioxidant enzymes, catalase (CAT) and superoxide dismutase (SOD), were used to map modulation of PEF-electrogenerated ROS.

RESULTS

PEF of buffer gave only weak, near to the background signal, chemiluminescence (data not shown), whereas BSA (Figure 1) produced a rising signal during the pulse train. Adding H_2O_2 strongly amplified pre-, during-, and post-pulsing signals in

REFERENCES

[1] Červinková K., *et al.* Modulation of pulsed electric field induced oxidative processes in protein solutions by proand antioxidants sensed by biochemiluminescence. *Sci rep*, 14:22649, 2024.

ACKNOWLEDGEMENTS

Authors acknowledge the support from the Czech Health Research Council, project n. NW25-08-00274.

Numerical modeling of unipolar intracardiac electrograms for assessing lesion transmurality after pulsed field ablation

Lana Balentović¹, Jernej Štublar^{1,2}, Tomaž Jarm¹, Lea Rems¹; Damijan Miklavčič¹; ¹University of Ljubljana, Faculty of Electrical Engineering, Tržaska 25, SI-1000 Ljubljana, SLOVENIA; ²University Medical Center, Zaloška cesta 7, SI-1000 Ljubljana, SLOVENIA

INTRODUCTION

Pulsed field ablation is an innovative method for treating atrial fibrillation that leverages irreversible electroporation to ablate arrhythmogenic myocardial cells. Achieving durable transmural lesions is essential for successful treatment and prevention of arrhythmia recurrence. Recently, unipolar intracardiac electrograms (iEGMs) have been suggested as a valuable tool for assessing lesion formation that could guide the ablation procedure [1].

The objective of this work was to construct a numerical framework to simulate iEGMs and investigate signal features that could facilitate the discrimination between transmural and non-transmural lesions.

METHODS

A two-dimensional rectangular domain measuring 20 mm \times 4 mm and representing a slab of cardiac tissue was constructed using COMSOL Multiphysics (Stockholm, Sweden). Single-cell electrical behavior and transmembrane voltage $(V_{\rm m})$ dynamics were described using the Luo-Rudy cardiomyocyte model [2]. An additional current was introduced to the original model, representing non-selective current flowing through membrane pores formed as a response to electric pulse exposure.

The cardiomyocyte model was coupled with the monodomain partial differential equation to simulate action potential (AP) propagation in the tissue. The iEGM signals were reconstructed during postprocessing by deriving the extracellular potential from the known transmembrane voltage distribution using Poisson's equation.

The simulation protocol involved applying a 2-millisecond rectangular stimulus to trigger AP propagation. Lesions of varying sizes were introduced, and iEGM signals were computed for each of nine equally spaced electrodes. The inter-electrode distance was set to 2 mm, and the center of the lesion was aligned with the position of electrode 6, as shown in Figure 1.

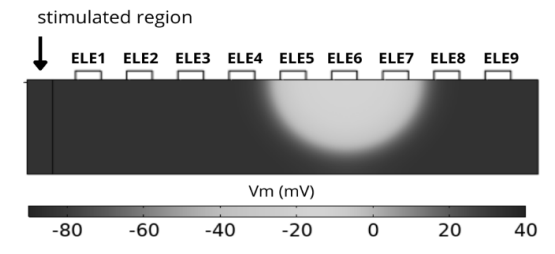


Figure 1: Model geometry with lesion site, electrode placement, and stimulated region.

RESULTS

Prior to the introduction of lesion, baseline simulations were conducted to validate monodomain model implementation. Signals on all electrodes exhibited physiologically consistent morphologies with appropriately delayed onsets. The presence of a lesion disrupted local AP propagation, causing the activation wavefront to divert around the lesion and distorting iEGM signals at nearby electrodes. As lesion size increased, distinct changes appeared in the ST and TQ segments, including S-wave attenuation and baseline shifts. For fully transmural lesions, the characteristic negative deflection disappeared, indicating complete conduction block beneath the electrode (Figure 2).

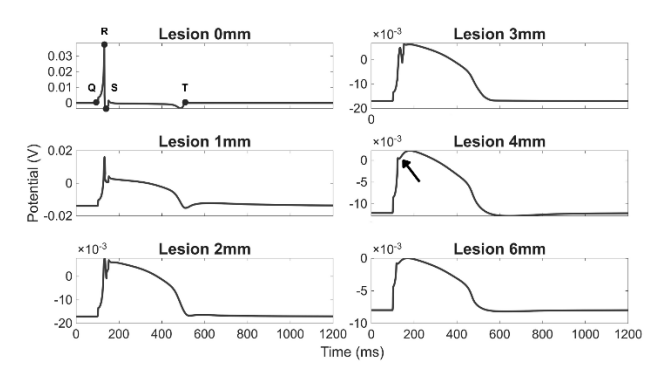


Figure 2: Changes in the unipolar iEGM signals recorded from the electrode positioned at the lesion centre. Points in the upper left panel indicate QRS complex and T-wave. Arrow denotes the loss of negative deflection following transmural lesion formation.

CONCLUSION

The model offers useful insight for interpreting iEGM changes during lesion formation, even though limited by its two-dimensional nature. Complete loss of the negative deflection observed in transmural lesions aligns with previously reported experimental findings supporting the use of unipolar iEGMs to guide ablation.

- [1] Yavin H. D., *et al.* Feasibility of unipolar signal—guided ablation in creating contiguous lines of conduction block:

 A proof-of-concept study. *Heart Rhythm*, S1547527125024336, 2025.
- [2] Luo C. H., *et al.* A model of the ventricular cardiac action potential. Depolarization, repolarization, and their interaction. *Circ Res*, 68:1501-1526, 1991.

Computational model of the electric field distribution in a 3D tissue mimic

Nyah M. Ebanks, Sam Salemizadeh Parizi, Zaid S. Salameh, Rafael V. Davalos; Wallace H. Coulter Department of Biomedical Engineering, Georgia Tech-Emory, Atlanta, GA 30318, USA

INTRODUCTION

Glioblastoma (GBM) is a malignant brain tumor that is both the most common and aggressive. The current GBM treatments yield a 5-year survival rate of 6.8%. The introduction of temozolomide, a chemotherapeutic agent, has increased the median survival rate from ~ 12.1 months to ~ 15 months. Although this therapy has improved the previous standard of care, the prognosis for GBM could be greatly improved [1].

Laser interstitial thermal therapy (LITT) is a thermal therapy that is minimally invasive. It uses an MRI-guided laser to ablate the GBM tumor tissue through heat. Since LITT deposits thermal energy into the brain, the tissues surrounding the tip undergo carbonization and charring [1].

Irreversible Electroporation (IRE) is a minimally invasive therapy that treats brain malignancies by targeting soft tissue using small surgical electrodes that deliver high-voltage, monophasic pulses [2]. IRE induces a non-thermal cell death mechanism which can improve the immune response [1].

The electric field distribution depends on the type and number of electrodes, as well as their position. This ensures that the electrodes will be able to induce cell death in the target region [3]. Here, using finite element analysis, we will model the effect of electrode spacing on the electric field distribution and map the lethal threshold.

METHODS

Using COMSOL Multiphysics (COMSOL, Stockholm, Sweden), we calculated the electric field distribution in a 3D hydrogel tissue mimic using previously established methods [4]. To investigate the effect of electrode spacing on field distribution we modeled two distance (3, 5 mm) while keeping voltage constant (500 V). The lethal electric field threshold for F98 brain cancer cells was pulled from Campelo et al. [1].

Table 1: Parameters for Hydrogel Numerical Model.

	,	
Parameter	Value	References
Hydrogel Conductivity	1.05 [S/m]	[4]
Electrode Conductivity	$4.03\times10^6\text{[S/m]}$	[4]
Hydrogel Radius	8 [mm]	Measured
Hydrogel Height	1.4 [mm]	Measured
Electrode Radius	0.36 [mm]	Measured
Electrode Spacing	3,5 [mm]	Varied
Voltage	500 [V]	[4]
Electric Field Threshold	845 [V/cm]	[1]

RESULTS

The numerical model displays the electric field distribution and lethal threshold in a F98 cell-hydrogel

mimic. Keeping the voltage at 500 V, the electrode spacing was varied (3, 5 mm). Figure 1a shows the electric field distribution for 3 mm electrode spacing. Figure 1b displays the electric field distribution for 5 mm electrode spacing. The lethal electrode becomes discontiguous as the spacing increases from 3 mm (Figure 1c) to 5 mm (Figure 1d).

As the electrode spacing increases, the electric field becomes less concentrated, and the threshold moves closer to electrode position. This model highlights the importance of scaling the voltage with electrode positioning when treating GBM to prevent gaps in treatment and tumor reoccurrence.

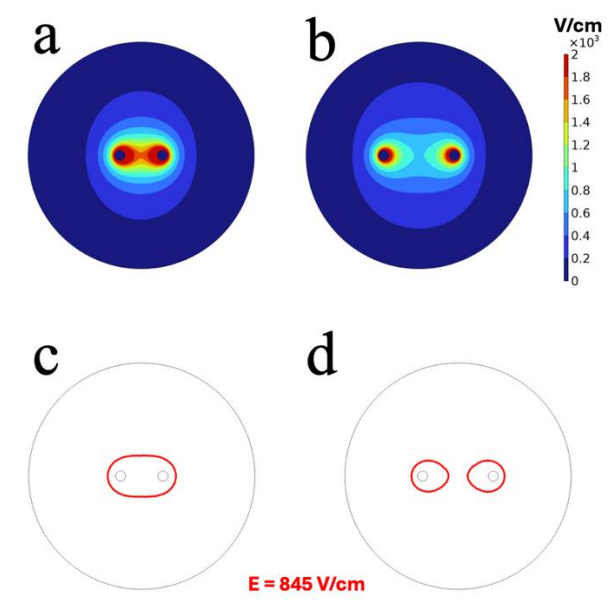


Figure 1: Numerical model of the electric field distribution in a F98 cancer cell-hydrogel tissue mimic. The electric field distribution of 3 mm **(a)** and 5 mm **(b)** spaced electrodes (V = 500V). The electric field threshold (red circle) for F98 cells in a 3 mm **(a)** and 5 mm **(b)** electrode spacing (V = 500V).

- [1] Campelo S. N., *et al.* High-frequency irreversible electroporation improves survival and immune cell infiltration in rodents with malignant gliomas. *Front Oncol*, 13:1171278, 2023.
- [2] Davalos R. V., *et al.* Tissue ablation with irreversible electroporation. *Ann Biomed Eng*, 33:223-231, 2005.
- [3] Aycock K. N., *et al.* A comparative modeling study of thermal mitigation strategies in irreversible electroporation treatments. *J Heat Transf*, 144:031206, 2022.
- [4] Campelo S. N., *et al.* Mitigating muscle contractions during pulsed field ablation by utilizing intersegment delays. *Bioelectrochemistry Amst Neth*, 166:109049, 2025.

Competing mechanisms for anisotropic lesion formation in cardiac PFA modelling

Argyrios Petras¹, Gerard Amoros Figueras², Zoraida Moreno Weidmann², Tomas Garcia Sanchez³, David Vilades Medel², Aurel Neic⁴, Edward J. Vigmond^{5,6}, Antoni Ivorra³, Jose M. Guerra², Luca Gerardo-Giorda^{1,7}; ¹Johann Radon Institute for Computational and Applied Mathematics (RICAM), Austrian Academy of Sciences, Linz, AUSTRIA; ²Hospital de la Santa Creu i Sant Pau, IR SANT PAU, Universitat Autonoma de Barcelona, CIBERCV, Barcelona, SPAIN; ³Department of Engineering, Universitat Pompeu Fabra, Barcelona, SPAIN; ⁴NumeriCor GmbH, Graz, AUSTRIA; ⁵Liryc Heart Rhythm Disease Institute, Fondation Bordeaux University, Bordeaux, FRANCE; ⁶CNRS, Bordeaux INP, IMB, University of Bordeaux, Bordeaux, FRANCE; ⁷Institute for Mathematical Methods in Medicine and Life Sciences, Johannes Kepler University, Linz, AUSTRIA

INTRODUCTION

Pulsed field ablation (PFA) is a novel cardiac ablation technology based on irreversible electroporation that has revolutionized the arrhythmia treatment. Despite its wide use, computational models are still unable to accurately capture the complex mechanisms of the lesion generation, thus not being able to capture the range of width-to-depth anisotropy ratio observed experimentally.

OBJECTIVE

This work aims to enhance our existing porcine open-chest computational model introduced in [1], to capture the wide range of the width-to-depth anisotropy ratio observed in experiments.

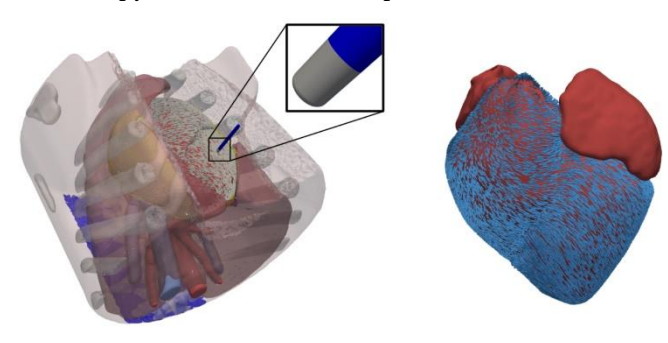
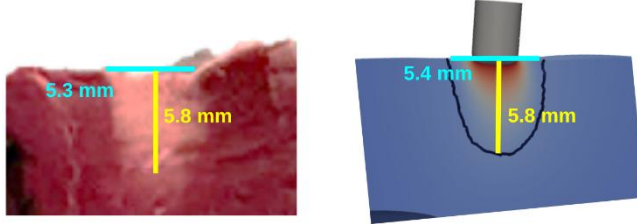


Figure 1: The porcine geometry from [1] incorporating cardiac fibres at the ventricles.

METHODS

We incorporate ventricular cardiac fibre orientations the open-chest geometry introduced in [1], using a rule-based algorithm (see Figure 1). Further, we consider two competing terms that alter the tissue electrical conductivity in an anisotropic manner: 1. An electroporation term that depends on the cardiomyocyte orientation, and 2. A gap junction

closure term that acts in the fibre direction. Lesion size was estimated using a lethal electric field threshold, and the resulting simulated lesions were compared



with experimental measurements reported in [1].

Figure 2: Simulated lesion (right) using the proposed model closely matches the shape of experimental lesion (left).

RESULTS

Incorporating the two competing mechanisms allows for a more accurate matching of the simulated lesion shape with the experimentally observed ones in [1] (Figure 2). By performing a sensitivity analysis, the gap junction closure term appears to be the second most important parameter (after the electric field lethal threshold) affecting the lesion shape.

CONCLUSION

The proposed model enables accurate simulations and lesion predictions that align with the experimentally observed results. The gap junction closure term is essential for predicting lesion shapes and should be incorporated into computational models.

REFERENCES

[1] Petras A., *et al.* Is a single lethal electric field threshold sufficient to characterize the lesion size in computational modeling of cardiac pulsed-field ablation? *Heart Rhythm O2*, 6: 671-677, 2025.

Assessing membrane permeabilization of Gram-negative bacteria using electrochemical impedance spectroscopy (EIS): differentiation from Gram-positive bacteria and evaluation of pulsed electric field (PEF) treatment efficacy, with and without antibiotics

Simona Gelažunaitė, Paulius Ruzgys, Mindaugas Visockis, Salvijus Vykertas, Saulius Šatkauskas; Institute of Natural Sciences and Technology, Vytautas Magnus University, Universiteto str. 10, Akademija, Kaunas District, LT-53361, LITHUANIA

INTRODUCTION

Understanding manipulating and bacterial membrane permeability is essential for developing non-chemical antimicrobial strategies and optimizing antibiotic efficacy. Electrochemical impedance spectroscopy (EIS) is a label-free, real-time, and nondestructive method that provides valuable insights into the dynamic changes in bacterial membranes, even in turbid or opaque media. This study examines the application of EIS to assess the outer membrane permeability of Gram-negative bacteria, distinguishing their response from that of Gram-positive bacteria, under Pulsed Electric Field (PEF) treatment and evaluating the synergistic effects of combining PEF with antibiotics.

METHODS AND RESULTS

Utilizing *Escherichia coli* (Gram-negative) and *Lactobacillus delbrueckii* subsp. *bulgaricus* (Grampositive) as model organisms, PEF treatments ranging from 4 to 16 kV/cm with pulse durations of 10×10 µs and 10×100 µs were applied. EIS measurements revealed that *E. coli* exhibited greater susceptibility to membrane permeabilization (Fig. 1) compared to *L. bulgaricus*, particularly at longer pulse durations, as indicated by significant changes in admittance magnitude and phase angle. These findings underscore EIS capability to effectively differentiate bacterial responses based on cell wall structure and PEF parameters [1].

In addition, we investigated the synergistic potential of combining PEF with the aminoglycoside antibiotics kanamycin and gentamicin. EIS data correlated with bacterial growth inhibition, showing that PEF significantly potentiated the effect of kanamycin against *E. coli*, especially during the first 3 h after treatment [2]. This suggests that PEF can potentiate antibiotic action, potentially allowing for lower antibiotic dosages while maintaining therapeutic effectiveness.

Bacterial detection in samples and the separation of Gram-negative and Gram-positive species remain a major analytical challenge, as traditional Gram staining is a labour-intensive and time-consuming method. Gnaim R. et al. (2020) aimed to evaluate the use of electrical bioimpedance spectroscopy (EBIS) as a low-cost, practical alternative for real-time bacterial detection and classification. The results showed that significant differentiation of bacterial types could be achieved by analysing the magnitude and phase of the impedance at frequencies of 158,489 Hz and 5,248 Hz,

respectively, at a bacterial concentration of 1 $\mu g/\mu l.$ Further analysis showed that the sensitivity of this method varied depending on the bacterial concentration. Overall, the results indicate that EBIS is a promising method for detecting the presence of bacteria and distinguishing between Gram-positive and Gram-negative species [3].

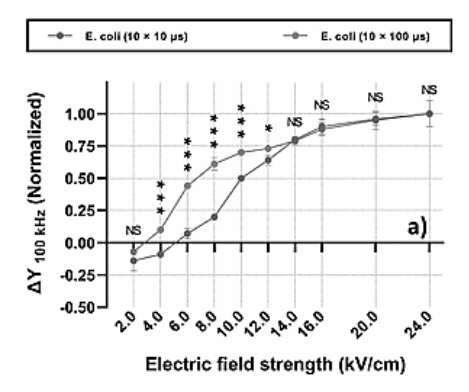


Figure 1: The mean values in admittance difference between untreated and PEF-treated samples against applied signal frequency for *E. coli*.

CONCLUSIONS

EIS has proven to be a sensitive tool for distinguishing between Gram-negative and Gram-positive bacterial responses to membrane-targeting interventions. Furthermore, the combination of PEF with aminoglycoside antibiotics significantly improves antibacterial efficacy, particularly with compounds like Kanamycin. These insights not only validate the utility of EIS in real-time assessment of bacterial membrane dynamics but also highlight the potential of combining physical and pharmacological treatments to enhance antimicrobial strategies.

- [1] Visockis M., *et al.* Application of pulsed electric field (PEF) as a strategy to enhance aminoglycosides efficacy against Gram-negative bacteria. *Bioelectrochemistry*, 164:108935, 2025.
- [2] Visockis M., et al. Detection of Gram-positive and Gramnegative bacteria membrane permeabilization induced by pulsed electric field using electrochemical admittance spectroscopy. Bioelectrochemistry, 161: 108835, 2024.
- [3] Gnaim R., *et al.* Detection and differentiation of bacteria by electrical bioimpedance spectroscopy. *BioTechniques*, 69:26-36, 2020.

Electroporation-based transformation of *Paenibacillus polymyxa*: effects of voltage on pEGFP uptake and kanamycin resistance

Aimal Waheed, Saulius Šatkauskas; Faculty of Natural Sciences, Vytautas Magnus University, Vileikos g. 8, 44404 Kaunas, LITHUANIA

INTRODUCTION

The Nitrogen fixing bacteria play a very important role in agriculture by minimizing the use of chemical fertilizers [1]. *Peanibacillus polymyxa*, a gram-positive bacterium, is used both as a biofertilizer and biocontrol. Genetic modification of *P. polymyxa*, through electroporation-based transformation techniques, allows for the enhancement of its functional genes to improve nitrogen fixation efficiency, increase biocontrol effectiveness, and adapt better to environmental stresses [2].

Electroporation is an effective method of introducing exogenous genes by increasing the membrane permeability via electrical pulses. In Grampositive species, optimal transformation accompanies balancing of electrical field strength to permeabilize the cell wall while maintaining the cell viability. The electric field intensity and pulse duration are vital for successful electroporation [3].

This study aims to optimize the voltage parameter (1,000–2,500 V, 5 ms pulse) for transforming *P. polymyxa* with a pEGFP plasmid carrying kanamycin resistance gene, cultured on LB agar at 37 °C. The voltage range was identified at which the transformation efficiency was at its peak, thus validating an electroporation protocol.

METHODS

Experiments were conducted on the gram-positive bacteria P.~polymyxa. plasmid Enhanced Green Fluorescent Protein (pEGFP) was introduced into the electrocompetent P~polymyxa cells using a decaying pulse ranging between 1000 V to 2500 V at 5 ms. The efficiency of the transfection was measured by counting the transfected cells on the kanamycin (50 μ g/mL) plates. The bacterial colonies grown after transfection on the antibiotic plates made sure that the bacteria acquired the plasmid and is now resistant to kanamycin.

RESULTS

The cell growth was first observed at 1200 V but the number of colonies was relatively low as compared to high electric field (1600 V-2200 V) where number of transfected colonies were significantly higher. So, at high electric field, more cells were transfected as the number of high-voltage (HV) pulses increased. At 1200 V almost 14% viable cells; at 1600 V, 30% viable cells; at 1900 V, 27% of cells; at 2000 V, 34% cells; at 2100 V, 50% of the cells were successfully transfected while the transfection rate peaked at 2200 V.

We also checked the transfection rate at relatively higher voltages like 2300 V-2500 V at 5 ms, but no colonies were observed in those parameters.

So, the viability of the cells was typically lower at both the extremes i.e. extremely high and extremely low. But it was optimal in the medium ranges i.e. 1600 V-2200 V.

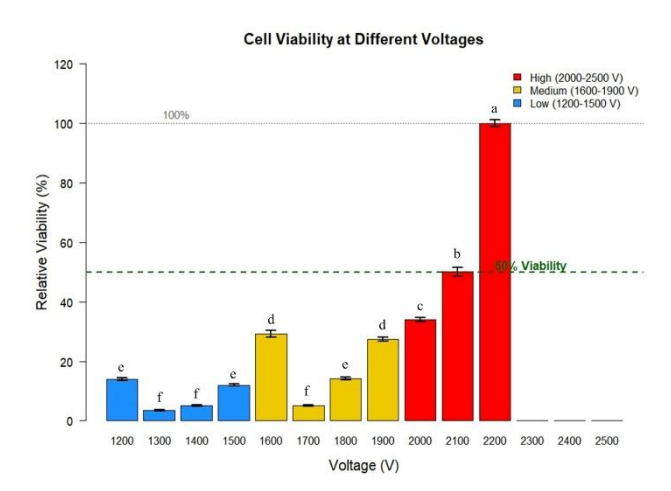


Figure 1: Relative cell viability (%) and colony formation across different electroporation voltages. Colony numbers are indicated for each condition. Blue markers represent low voltage (<1600 V), yellow markers medium voltage (1700–2000 V), and red markers high voltage (\geq 2100 V). The dashed red line indicates the 50% viability threshold.

CONCLUSION

Our findings suggest that the Gram-positive bacteria *P. polymyxa* does not acquire any plasmid at low pulses. However, as the electric field strength was enhanced, the optimal transfection rate started to increase while maintaining optimal cell viability. We also found that extremely high pulses decrease the cell viability thus electroporation of *P. polymyxa* in a range of 1600 V-2200 V is optimum for both transfection efficiency and cell viability.

- [1] Massey M. S., *et al.* Beyond soil inoculation: Cyanobacteria as a fertilizer replacement. *Nitrogen*, 4:253-262, 2023.
- [2] Li Q., *et al.* Nitrogen fixation by *Paenibacillus polymyxa* WLY78 is responsible for cucumber growth promotion. *Plant and Soil*, 473:507-516, 2022.
- [3] Löfblom J., et al. Optimization of electroporationmediated transformation: Staphylococcus carnosus as model organism. J Appl Microbiol, 102:736-747, 2007.

Non-uniformity of pulsed electric field treatment effects on plant tissues as evidenced by magnetic resonance imaging methods

Madita Kirchner^{1,2}, Marko Stručić³, Igor Serša⁴, Claudia Siemer¹, Damijan Miklavčič³, Stefan Toepfl^{1,5}, Samo Mahnič-Kalamiza³; ¹Elea Technology GmbH, Niedersachsenstr. 5, 49610 Quakenbrueck, GERMANY; ²Institute of Food Technology, University of Natural Resources and Life Sciences, Muthgasse 18, 1190 Vienna, AUSTRIA; ³Faculty of Electrical Engineering, University of Ljubljana, Tržaška c. 25, 1000 Ljubljana, SLOVENIA; ⁴Jožef Stefan Institute, Jamova c. 39, 1000 Ljubljana, SLOVENIA; ⁵University of Applied Sciences Osnabrueck, Albrechtstr. 30, 49076 Osnabrueck, GERMANY

INTRODUCTION

Pulsed Electric Field (PEF) treatment is a non-thermal technology for improving process efficiency and product quality in plant-based food production. While widely used in the potato processing industry [1], its broader application is challenged by non-uniform effects in structurally complex plant matrices [2]. MRI, specifically T_2 relaxation mapping, offers spatially resolved insights into water dynamics post-PEF [3], addressing gaps in understanding tissue-specific responses. This study aims to characterize the spatial non-uniformity of PEF effects across selected plant tissues using MRI T_2 mapping, addressing tissue orientation and structure.

MATERIALS AND METHODS

Five plant materials (sweet potato, potato, carrot, red beet, and broccoli) were subjected to PEF treatments at varying field strengths (0.2 to 3 kV/cm), pulse numbers (10 to 90), and orientations (parallel/perpendicular to tissue structure). T_2 mapping was performed before and up to 12 hours after treatment to visualize and quantify spatial tissue responses.

RESULTS

Results revealed tissue-specific and region-dependent PEF effects. Sweet potato exhibited different T_2 changes in xylem and parenchyma, while in potato, differences between inner and outer medulla pointed to starch-mediated water retention effects. In carrot, an increase (Fig. 1A, 1B) or homogenization (Fig. 1C, 1D) of T_2 times between cortex and xylem was determined after PEF treatment, while red beet maintained structural inhomogeneity between its layered cambium rings. Broccoli showed strong orientation-dependent changes, particularly in more lignified areas.

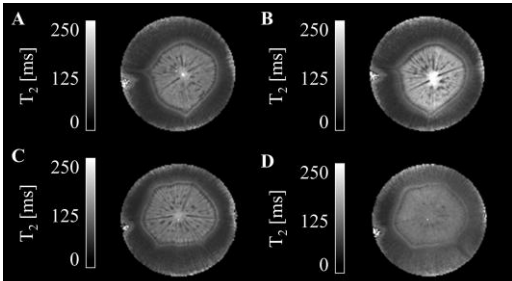


Figure 1: T_2 relaxation time maps of two carrot samples. (A, B) First carrot: (A) untreated, (B) after treatment at 1 kV/cm

with 10 pulses. (C, D) Second carrot: (C) untreated, (D) after treatment at $1.75\,kV/cm$ with 30 pulses.

Across samples, an initial change in T_2 time was often followed by apparent partial or full tissue homogenization when increasing treatment intensities or extending time between treatment and imaging (Fig. 2). In highly starchy tissues, T_2 mapping may have limited suitability to fully describe water dynamics, suggesting a need for complementary analytical methods.

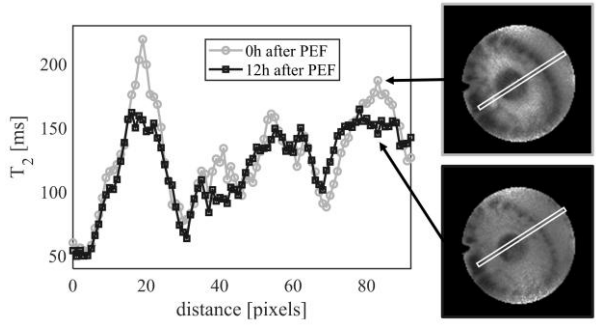


Figure 2: T₂ relaxation time profiles of a red beet sample measured along the indicated line immediately and 12 h after PEF treatment (1.75 kV/cm, 30 pulses).

CONCLUSION

These findings highlight the critical role of tissue structure, composition, and field orientation in determining PEF efficacy. MRI-based T_2 mapping proves to be a valuable, non-invasive tool for elucidating spatial PEF effects and guiding the development of more precise, material-specific treatment protocols, supporting the design of sustainable, high-quality food processing strategies.

- [1] Hill K., *et al.* Pulsed electric fields in the potato industry. in *Food Engineering Series*. Cham: Springer, 325-335, 2022.
- [2] Pataro G., *et al.* Limitations of pulsed electric field utilization in food industry," in *Pulsed electric fields to obtain healthier and sustainable food for tomorrow.* Amsterdam: Elsevier, 283-310, 2020.
- [3] Genovese J., et al. PEF treatment effect on plant tissues of heterogeneous structure no longer an enigma: MRI insights beyond the naked eye. Food Chem, 405, 2023.

Characterising H9c2 cell electroporation susceptibility in suspension and monolayer cultures

Aras Rafanavicius, Saulius Satkauskas; *Faculty of Natural Sciences, Vytautas Magnus University, Universiteto 10, LT-53361 Akademija, LITHUANIA*

INTRODUCTION

Electroporation is a widely utilised technique with growing interest in clinical applications such as tissue ablation, particularly for cardiac arrhythmias [1]. Its efficacy and safety are highly dependent on precisely controlled electric field parameters, which directly transition influence the between electroporation (RE), resulting in cell survival and transient membrane permeabilization, and irreversible membrane permeabilization (IRE), leading to cell death. Despite its widespread application on a variety of cell cultures, including the H9c2 cardiac myoblast cell line, there remains a notable scarceness of reliable, systematically generated data defining the precise electroporation thresholds for these distinct treatment outcomes [2]. This knowledge gap necessitates trialand-error optimisation for each specific experimental setup, hindering reproducibility and efficiency.

METHODS

This investigation addresses this need characterizing H9c2 cardiac myoblast cell susceptibility to electroporation under different culture conditions. Here, the cells were suspended in HEPES-based electroporation medium and subjected to single 100 us pulses with electric field strength varying from 200 to 3600 V/cm. RE and IRE were assessed via flow cytometry, utilising the membrane-impermeant fluorescent probe propidium iodide (PI), added either prior to electroporation for RE evaluation or 20 min post-pulse for IRE quantification. In parallel, monolayer electroporation efficiency was studied. H9c2 cells were seeded into 24-well plates (90000 cells/well) and, 24 h post-incubation, treated with 2, 5 or 10 100 us pulses of 280 V. RE and IRE were determined through fluorescence microscopy using PI, with the affected area measurements performed to quantify permeabilized regions.

RESULTS AND CONCLUSIONS

Our findings from suspension cultures reveal an initial threshold for PI electrotransfer at about 800 V/cm with notable increase in PI fluorescence observed from 1000 V/cm upwards. Correspondingly, irreversible membrane damage was detected under these conditions, although cell fluorescence remained relatively low even at single 3600 V/cm pulses.

In monolayer culture experiments, the affected areas have been determined, with the IRE/RE ratio reaching about 30%. Notably, comprehensive detection of irreversibly damaged cells proved more challenging than expected due to sensitivity of the cells to mechanical perturbations during experimental preparations and relatively low PI fluorescence exhibited by the cells within the supposedly treated areas.

These results provide initial insights into H9c2 cell culture electroporation dynamics, critical for further development of targeted pulsed field ablation-based strategies.

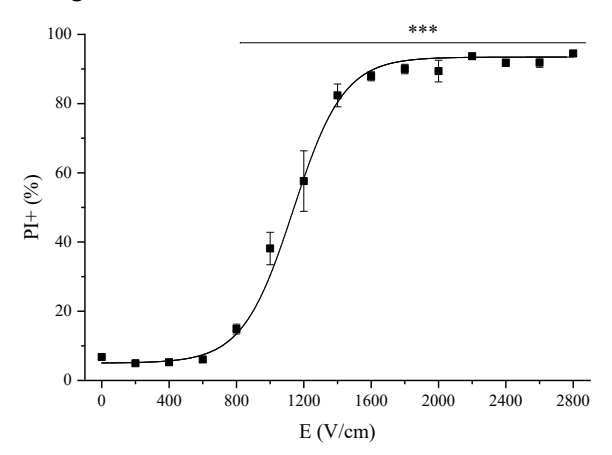


Figure 1: Dependence of PI-positive cells on electric field strength.

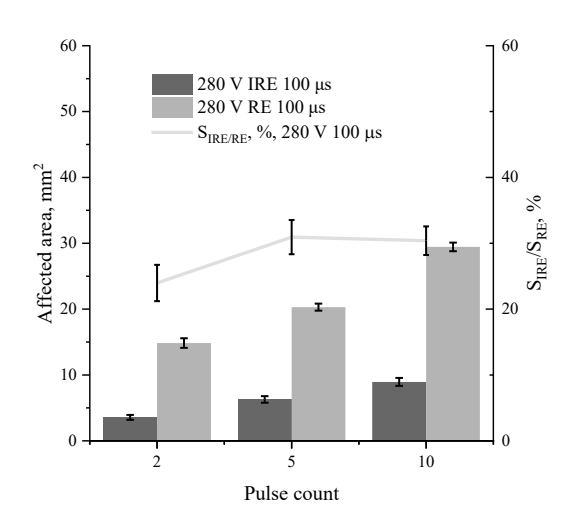


Figure 2: Monolayer IRE and RE areas and the IRE/RE area ratio.

- [1] Schaack D., *et al.* Pulsed field ablation for atrial fibrillation. *AER*, 12:e11, 2023.
- [2] Xuying Y., et al. Study on optimal parameter and target for pulsed-field ablation of atrial fibrillation. Front Cardiovasc Med, 8:690092, 2021.

Advances in irreversible electroporation and elucidating cell death pathways

Kailee M. David, Edward Jacobs IV, Rafael V. Davalos; *Department of Biomedical Engineering, Georgia Tech, Atlanta, GA 30318*, *USA*

INTRODUCTION

Irreversible Electroporation (IRE) is a minimally invasive tissue ablation technique that involves applying low-energy pulses to create defects in the lipid bilayer, inducing cell death. [1]. IRE is unique among ablation techniques in affecting only the cell membrane while tissue molecules such as collagen structures and proteins remain intact, thereby making treatment near critical structures possible. We developed an advanced form of the technology, high frequency irreversible electroporation (H-FIRE) [2], that is being used for the treatment of cardiac disease, cancer and other malignancies. This new therapy alleviates the need for a paralytic.

Different waveforms and fields elicit different cell death mechanisms, including necrosis, apoptosis, pyroptosis, necroptosis, and ferroptosis [3]. These pulses have been shown to increase antigen activity with the release of damage associated molecular pathways (DAMPs) and proteins [4]. By modifying the pulse parameters and field strength, specific modes of cell death can be triggered [5]. We will discuss such mechanisms and modeling techniques to avoid thermal damage. We will also discuss recent advances in pulsed electric field therapies to target other aspects of the tumor microenvironment and potential clinical applications.

METHODS

A pancreatic cancer cell line, Panc-1, was seeded into a 3D collagen hydrogel platform used for electroporation treatments. At a 6-hour time point, ablation areas (n=3) were imaged using a live immunofluorescent stain and confocal microscopy to visualize the area of cell death indicated by a lack of mitochondrial activity as well as the area in which apoptotic cell death indicated by Caspase 3 activation is occurring.

RESULTS

We found that Caspase 3 activation (Figure 1) increased with increasing ablation area and pulse width. At the 6-hour peak time point of apoptotic death, previously determined by Mercadal et al. [3], a heightened green, fluorescent signal is seen throughout the ablation area. These results indicate that apoptotic and necrotic cell death can both occur in the central area of the ablation.

CONCLUSION

We determined that multiple cell death mechanisms can contribute to the ablation area in the same regions.

By applying the same voltage for different waveforms, we see that apoptosis occurs in all cases within the previously denoted "necrotic zone", implying that crosstalk between apoptotic and necrotic cell death processes may be contributing to the entirety of the ablation area. With this information, we can develop treatment plans to control the area in which an immune response to therapy occurs to optimize patient recovery times and overall survival.

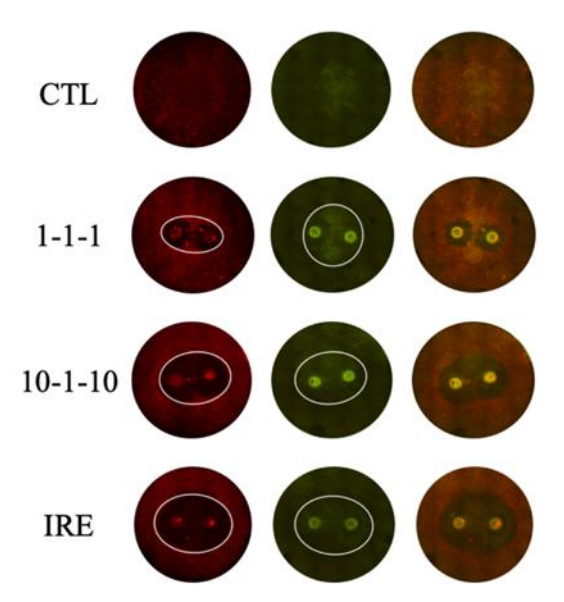


Figure 1: Immunofluorescent confocal microscopy images of mitochondrial activity (red channel), Caspase 3 activation (green channel), and the combined channels.

- [1] Davalos R. V., *et al.* Tissue ablation with irreversible electroporation. *Ann Biomed Eng*, 33:223-231, 2005.
- [2] Arena C. B., et al. High-frequency irreversible electroporation (H-FIRE) for non-thermal ablation without muscle contraction. Biomed Eng Online, 10, 2011
- [3] Mercadal B., *et al.* Dynamics of cell death after conventional IRE and HFIRE treatments. *Ann Biomed Eng*, 48, 2020.
- [4] Ringel-Scaia V. M., *et al.* High-frequency irreversible electroporation is an effective tumor ablation strategy that induces immunologic cell death and promotes systemic anti-tumor immunity. *EBioMedicine*, 44, 2019.
- [5] Polajžer T., *et al.* Immunogenic cell death in electroporation-based therapies depends on pulse waveform characteristics. *Vaccines*, 11, 2023.

Impact of vascular lock on blood flow distribution under pulsed electric fields: experiments and simulations

Elisabeth Bellard, Sandrine Pelofy, Marie-Pierre Rols, Justin Teissié, **Maxime Berg** and Muriel Golzio; *Institut de Pharmacologie et de Biologie Structurale, Université de Toulouse, CNRS, Toulouse. FRANCE*

INTRODUCTION

Pulsed electric fields are the cornerstone of electrochemotherapy (ECT) and electrogenotherapy (EGT) [1]. Such fields leverage both electroporating and electrophoretic processes to dramatically improve drug and plasmid delivery to the target cells, addressing one major bottleneck of drug delivery [2]. Although the properties of pulsed electric fields (location, pulse intensity and pulse duration) can be finely tuned, such fields still affect all tissue structures within reach, including the microvasculature. In particular, they induce a transient vasoconstriction of blood vessels, known as vascular lock [3].

While short-lived, this phenomenon severely disrupts the underlying blood flow distribution. The interconnected nature of the microvascular system, which is inherently multiscale and non-local, makes it difficult to quantify the impact of vascular lock both spatially (the extend of region affected) and in time (relaxation in arterioles, capillary and venules), with uncharted consequences for therapeutic processes.

METHODS

To address this, we combined intravital microscopy on mice with mathematical modelling to decipher the cross-talk between pulsed electric fields, vascular lock and blood flow dynamics.

Dorsal window chambers were surgically placed on an extended double layer of skin, enabling direct access to dermis microvasculature [4]. Microsecond pulsed electric fields were applied to the skin. Following the pulses, variations of labelled red blood cell velocities were measured via fluorescence video microscopy in venules. Variations of the associated diameters in both arterioles and venules were measured using contrast between surrounding tissue and vessel lumen.

Vascular dynamics was modelled using a porenetwork approach [5]. The model accounted for both the complex rheology of the blood at the microscale and the transient variation of vessel diameters [6]. Arteriovenular tree properties were derived from imaging while the capillary bed was built using model Voronoi diagrams. Intravascular pressure and blood flow rate were solved, using arteriolar diameter variations as input and venular diameter and red blood cell velocities as validating output.

RESULTS AND DISCUSSION

In doing so, we show that vascular lock effect lasted upward to 10 minutes following the microsecond pulses affecting arterioles and venules alike, with some arterioles being completely obstructed. Further, our model was able to reproduce the blood flow dynamics observed in venules, including reversal in flow

direction at early time point (Figure 1) that we linked to vessel compliance in the model. At the capillary level, simulations highlighted dynamic heterogeneities, with regions of low perfusion and stalling correlating with longer travel times potentially allowing for better exchanges with the surrounding tissue.

Our results therefore indicate the existence of an unsuspected therapeutic window following vascular lock which has the potential to be hacked to improve delivery during ECT and EGT.

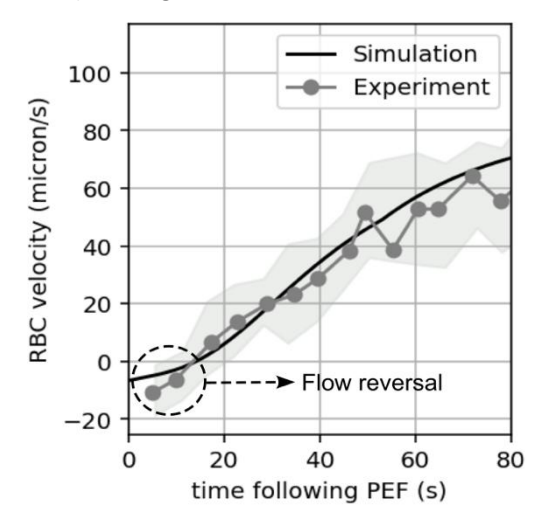


Figure 1: Measured and predicted red blood cell velocity in venules during transient vascular lock.

- [1] Yarmush M. L., *et al.* Electroporation-based technologies for medicine: principles, applications, and challenges. *Annu Rev Biomed Eng*, 16:295-320, 2014.
- [2] Chabot S., et al. Targeted electro-delivery of oligonucleotides for RNA interference: siRNA and antimiR. Adv Drug Del Rev, 81:161-168, 2015.
- [3] Jarm T., et al. Antivascular effects of electrochemotherapy: implications in treatment of bleeding metastases. Expert Rev Anticancer Ther, 10:729-746. 2010.
- [4] Bellard E., *et al.* Intravital microscopy at the single vessel level brings new insights of vascular modification mechanisms induced by electropermeabilization. *J Control Release*, 163:396-403, 2012.
- [5] Merlo A., *et al.* A few upstream bifurcations drive the spatial distribution of red blood cells in model microfluidic networks. *Soft Matter*, 18:1463-1478, 2022.
- [6] Reichold J., et al. Vascular graph model to simulate the cerebral blood flow in realistic vascular networks. *JCBFM*, 29:1429-1443, 2009.

In vitro evaluation of pulsed field ablation-induced hemolysis using bovine blood in a benchtop model

James P. Villar-Mead^{1,2,3}, Sindu Thinamany⁴, Lars M. Mattison⁴, Tugba Kumru⁴, Gary R. Fiedler⁴, Daniel C. Sigg⁴, Paul A. Iaizzo^{1,2,3}; ¹Department of Biomedical Engineering and Surgery, USA; ²Institute for Engineering in Medicine, USA; ³Visible Heart Laboratories, University of Minnesota, Minnesota, USA; ⁴Medtronic, Minnesota, USA

INTRODUCTION

Pulsed field ablation (PFA) is the application of irreversible electroporation (IRE) to create pores in cellular membranes, subsequently leading to loss of ion homeostasis and cell death [1]. Red blood cells (RBC) are susceptible to electroporation, with pore formation leading to hemolysis [2]. RBC hemolysis can cause systemic effects after PFA procedures used to treat cardiac arrythmias such as acute renal injury [3]. Therefore, optimization of PFA waveform parameters to maximize lesion formation while minimizing collateral blood damage needs to be investigated further.

METHODS

Bovine blood samples were homogeneously mixed using a V&P Scientific SpinVessel® 350 mL motor system (VP 418SV3-1-350RB-CC, San Diego, CA, United States). Two parallel bipolar electrodes separated by 1 cm, were inserted into the center of an isolated blood volumes (300mL). Varying biphasic pulse widths (500ns, $2\mu s$, $8\mu s$) were adjusted while keeping the voltage, interphase delay, interpulse delay, pulses, and pulse trains constant (1400V, $2\mu s$, $100\mu s$,

(mPOR, L-POR V 1.1, Ljubljana, Slovenia).

Blood samples (6mL) were drawn from the SpinVessel following 0,2,4,8,16 ablation applications and subsequently centrifuged. The plasma samples were then pipetted and analyzed for hemolysis via Blakney and Dinwoodie spectrophotometric scanning technique [4].

RESULTS

It was observed that 500 nanoseconds, being the shortest pulse width tested, elicited the lowest amount of hemolysis in an isolated blood pool: with increasing hemolysis correlating with increases to pulse widths (Figure 1).

CONCLUSION

The utilization of this in vitro benchtop model provided reproducible testing of the effects of PFA-induced hemolysis of RBC. Planned future experiments with varying waveform parameters, cell death curves, and electrode configurations will provide additional insights into these processes.

- [1] Jacobs E. J., *et al.* Pulsed field ablation in medicine: irreversible electroporation and electropermeabilization theory and applications. *Radiol Oncol*, 59:1-22, 2025.
- [2] Popa M. A., *et al.* Characterization and clinical significance of hemolysis after pulsed field ablation for atrial fibrillation: Results of a multicenter analysis. *Circ Arrhythm Electrophysiol*, 17, 2024.
- [3] Martinez J., *et al.* Renal safety of high dose pulsed field ablation of atrial fibrillation: a prospective real-world analysis *Heart Rhythm*, 2025.
- [4] Blakney G. B., *et al.* A spectrophotometric scanning technique for the rapid determination of plasma hemoglobin. *Clin Biochem*, 8:96-102, 1975.

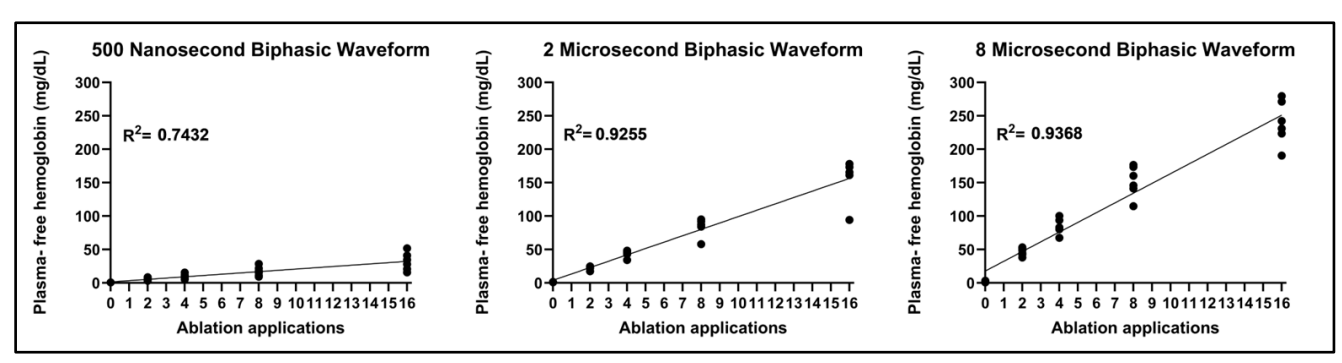


Figure 1: Ablation application-dependent PFA-induced hemolysis measured by plasma free hemoglobin levels. Each point represents an individual measurement at each application (n=6,5,6).

Localized coronary vasospasm and flow velocity changes following pulsed field ablation

Álvaro Borachok ^{1,*}, Gerard Amorós Figueras^{1,*}, Quim Castellví², Sergi Casabella-Ramon¹, Marc Soriano-Amores¹, Antoni Ivorra^{2,3}, Jose M Guerra¹; ¹Department of Cardiology, Hospital de la Santa Creu i Sant Pau, Institut de Recerca Sant Pau (IR Sant Pau), CIBERCV, Universitat Autònoma de Barcelona, Barcelona, SPAIN; ²Department of Engineering, Universitat Pompeu Fabra, Barcelona, SPAIN; ⁸Serra Húnter Fellow Programme, Universitat Pompeu Fabra, Barcelona, SPAIN. * Both authors contributed equally

INTRODUCTION

Pulsed field ablation (PFA) has emerged as a therapeutic technique promising for cardiac arrhythmias. Its mechanism relies on irreversible electroporation, which induces permanent nonconductive lesions that block abnormal conduction pathways [1]. However, when applied near coronary arteries, PFA can induce acute coronary vasospasm, as reported in both clinical and preclinical studies [2]. The physiological impact of these spasms on coronary blood flow remains poorly characterized. We hypothesized that PFA-induced vasospasm near the left anterior descending coronary artery (LAD) alters coronary flow velocity.

OBJECTIVE

To detect blood flow velocity changes in the coronary arteries induced by PFA-induced vasospasm by using a coronary flowprobe.

METHODS

The study involved 4 domestic swine weighing 59 \pm kg. Animals were anesthetized and analgesia administered as described in [3]. The thorax was exposed, and the heart was suspended in a pericardial cradle. Two femoral arteries were catheterized and a guiding catheter was advanced under fluoroscopic control to the proximal part of the LAD. We continuously measured the coronary flow using a flowprobe that was carefully placed over the distal part of the LAD (Figure 1A). The arterial pressure was also monitored using the other femoral access and the surface ECG (avL) continuously recorded. Then, an epicardial site directly over the proximal part of the LAD was selected and approx. 20 ml of contrast agent was injected via the guiding catheter to perform a baseline angiography. A PFA application (burst frequency 450 kHz, Vpp=2 kV) was performed on the targeted site and we immediately repeated the angiography after the application. After complete recovery of the observed vasospasm, a new location directly over the LAD was selected and the procedure was repeated. We classified the PFA application locations depending on their distance to the flowprobe as: "far" if they were >1cm from it, or "near" if ≤ 1 cm from it.

RESULTS

Vasospasm was confirmed in all PFA applications over the LAD. No significant changes in coronary flow velocity were observed when PFA lesions were placed far from the flow probe (flow_pre vs. post: 14.47 ± 5.86

ml/min vs. 15.36 ± 4.71 ml/min; p=ns) (Figure 1B). In contrast, applications near the sensor resulted in detectable pre- to post-PFA differences (flow_pre vs. post: 15.48 ± 4.56 ml/min vs. 28.30 ± 2.57 ml/min; p<0.05), likely due to localized flow acceleration caused by coronary narrowing during the vasospasm, consistent with fluid dynamics predictions [4].

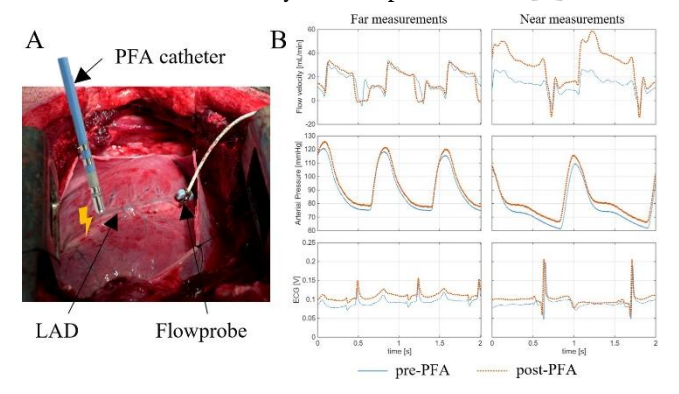


Figure 1: A. Experimental setup. B. Flow velocity (top row), arterial pressure (middle), and ECG (bottom) for far (left column) and near (right) measurements.

CONCLUSIONS

PFA-induced vasospasm near LAD can transiently alter coronary flow velocity, likely due to localized narrowing, but these blood flow velocity changes are only detectable when measured very near the induced vasospasm.

- [1] Verma A., *et al.* Primer on pulsed electrical field ablation. *Circ: Arrhythmia Electrophysiol*, 14, 2021.
- [2] Tam M. T. K., *et al.* Effect of pulsed-field ablation on human coronary arteries: a longitudinal study with intracoronary imaging. *JACC Clin Electrophysiol*, 11:1478-1488, 2025.
- [3] Amorós-Figueras G., *et al.* Dynamics of high-density unipolar epicardial electrograms during PFA. *Circ: Arrhythmia Electrophysiol*, 16, 2023.
- [4] Edrisnia H., *et al.* Non-invasive fractional flow reserve estimation in coronary arteries using angiographic images, Sci Rep, 14:15640, 2024.
- [5] Klein N. *et al.* The combination of electroporation and electrolysis (E2) employing different electrode arrays for ablation of large tissue volumes. *PLoS ONE*, 14:1-13, 2019.

Engineering of plasmids expressing bacterial toxins for in situ cancer vaccination

Maja Cvetanoska^{1, 2}, Kristijan Lovišček³, Katarina Žnidar¹, Maja Čemažar^{1, 4}, Gregor Serša^{1, 5}, Urška Kamenšek^{1, 3}; ¹Department of Experimental Oncology, Institute of Oncology Ljubljana, SLOVENIA; ²Faculty of Medicine, University of Ljubljana, SLOVENIA; ³Biotechnical Faculty, University of Ljubljana, SLOVENIA; ⁴Faculty of Health Sciences, University of Primorska, Izola, SLOVENIA; ⁵Faculty of Health Sciences, University of Ljubljana, SLOVENIA

INTRODUCTION

In situ cancer vaccination offers a promising strategy to turn the tumor itself into an endogenous source of antigens, thereby enabling immune-mediated tumor eradication [1]. We are developing a plasmid-based gene therapy platform that delivers secreted forms of bacterial toxins via gene electrotransfer (GET) to activate antitumor immunity directly within the tumor microenvironment. Our strategy combines pore-forming toxins (PFTs), designed to lyse tumor cells and release antigens [2], with superantigen toxins (SAgs), intended to amplify local immune activation [3].

METHODS

To select the most suitable toxin candidates and eukaryotic secretion signals, we first performed an extensive literature review. Toxin coding sequences were retrieved from nucleotide databases, codonoptimized for mammalian expression, and fused to upstream secretion signals. In parallel, reporter constructs with green fluorescent protein (GFP) were designed to evaluate secretion efficiency. All constructs were synthesized de novo, inserted into mammalian expression vectors, and validated by restriction digestion and whole-plasmid sequencing. For functional evaluation, transfection-grade plasmid DNA was delivered into B16-F10 murine melanoma cells using GET (8 x 260 V/2mm, 100 $\mu s,\,1\,Hz).$ At 48 hours post-transfection, secretion signal functionality was assessed by quantifying intracellular and extracellular GFP fluorescence, and toxin gene expression was evaluated by qRT-PCR. Cell viability was also assessed at 72 h post-transfection using PrestoBlue to evaluate the cytotoxicity of the toxinencoding plasmids.

PRELIMINARY RESULTS

We successfully generated five plasmids encoding pore-forming toxins (PFTs): Escherichia coli cytolysin A and Shiga toxin 2, Streptococcus pyogenes streptolysin O, Aeromonas hydrophila aerolysin, and Staphylococcus aureus alpha-hemolysin and three plasmids encoding superantigens (SAgs): S. aureus enterotoxins A and B, as well as toxic shock syndrome toxin-1 (TSST-1). All toxin genes were fused to the perforin-1 secretion signal. Reporter plasmids with green fluorescent protein (GFP) were also successfully generated to evaluate secretion efficiency. Following GET into target cells, the proportion of GFP-positive cells was quantified and compared among the three GFP-expression plasmids: pEGFP-N1, pCMV-sEGFP-PRF1 and pCMV-sEGFP-IL2 and toxin gene expression was confirmed by qRT-PCR.

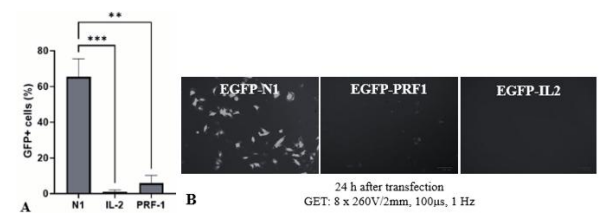


Figure 1: A) Percentage of GFP* B16-F10 cells 48 h after transfection with the following plasmids: pEGFP-N1 (a commercial plasmid for expressing GFP without a secretion signal), pCMV-sEGFP-PRF1 (a plasmid for expressing GFP with the secretion signal of the perforin 1 gene) and pCMV-sEGFP-IL2 (a plasmid for expressing GFP with the secretion signal of the interleukin 2 gene).

B) Fluorescence microscopy images of GFP expression 24 h after transfection with the following plasmids: pEGFP-N1, pCMV-sEGFP-PRF1 and pCMV-sEGFP-IL2.

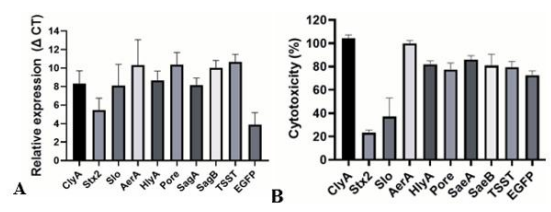


Figure 2: A) Relative toxin gene expression in transfected B16-F10 cells **B)** Cytotoxicity of toxin-expressing plasmids in B16-F10 cells.

CONCLUSION

The results presented in this abstract are preliminary, and further experiments will be needed to fully confirm the basic functionally of the newly prepared plasmids. Furthermore, future functional assays will be essential to determine whether toxins secreted from transfected tumor cells, rather than their bacterial counterparts, retain effective pore-forming and superantigenic activities.

- [1] Hammerich L., *et al.* In situ vaccination: cancer immunotherapy both personalized and off-the-shelf. *Mol Oncol*, 9:1966-1981, 2015.
- [2] Pahle J., et al. Bacterial toxins for oncoleaking suicidal cancer gene therapy. Recent Results Cancer Res, 209:95-110, 2016.
- [3] Torres B. A., *et al.* Superantigens: The good, the bad, and the ugly. *EBM*, 226:164-176, 2001.

Production and functional assessment of recombinant gelonin for electroporation applications

Eleni Zivla, Andrei G. Pakhomov, Olga N. Pakhomova; Frank Reidy Research Center for Bioelectrics, Old Dominion University, Norfolk, VA 23508, USA

INTRODUCTION

Ribosome-inactivating proteins (RIPs) are toxins inhibiting eukaryotic protein synthesis by depurating a specific adenine residue in 28S rRNA [1]. Gelonin, a Type I RIP from Gelonium multiflorum, is highly potent toxin but lacks cell-entry mechanisms and remains non-toxic therefore under normal physiological conditions. We previously demonstrated that pulsed electric fields (PEF) facilitate gelonin uptake and enhance its cytotoxicity by several thousand-fold, bringing EC_{50} values to the low-nanomolar range [2]. In the presence of 100 nM gelonin, the PEF dose required for effective cell death decreases at least tenfold, demonstrating strong synergy and supporting gelonin's potential as an electrochemotherapy agent alongside bleomycin and cisplatin.

In this work, we established an *E. coli*-based expression system and an HPLC-controlled purification protocol for recombinant gelonin (rGel). This in-house production enables precise sequence control, facilitates structural modification and labeling, and provides a reliable and cost-effective protein supply.

METHODS

A DNA fragment encoding residues 47–296 of gelonin was fused to a DNA sequence coding for tobacco etch virus (TEV) protease recognition site and cloned into the pET-32a(+) vector between the XhoI and KpnI restriction sites. The resulting construct encoded for recombinant gelonin (rGel) fused to an attachment upstream of rGel sequence, comprising a thioredoxin (Trx) domain to promote solubility and folding, a 6His tag for affinity purification, and a TEV site enabling removal of the fusion partners without residual amino acids at the rGel N-terminus.

The pET32a-rGel plasmid was transformed into $E.\ coli\ BL21(DE3)$ cells, and ampicillin-resistant clones were selected and cultured in LB medium (100 µg/mL Amp) at 37 °C. Protein expression was induced at OD₆₀₀ \approx 0.4 with 0.5 mM IPTG, followed by overnight incubation at 23 °C. Cells were lysed by sonication on ice, and the clarified lysate was loaded onto a Ni²+affinity column. Trx-6His-rGel was eluted with a 20–500 mM imidazole gradient, and peak fractions were pooled and digested overnight with TEV protease (15:1, w/w). The digest was passed through a second Ni²+affinity column to remove 6His-tagged fragments (6His-Trx and 8His-TEV), while untagged rGel was recovered in the flow-through.

Endotoxins were removed using an endotoxinspecific affinity matrix, and rGel was further purified by cation-exchange chromatography. Protein purity and molecular weight were verified by SDS-PAGE. Ribosome-inactivating activity was assessed using a cell-free translation assay with a GFP reporter, and cytotoxicity was evaluated in CT26 cells exposed to pulsed electric fields ($8 \times 100 \, \mu s$, $1.1 \, kV/cm$).

RESULTS

Recombinant gelonin was successfully expressed in $E.\ coli$ and purified using an automated HPLC-controlled workflow, with consistent quality and reproducibility. The endotoxin level was below 2 EU/mg, within FDA limits for safe I.V (< 2.8 mg/kg) and intratumoral (< 71 µg) administration in mice. Native plant-derived gelonin (nGel) and rGel show similar translation-inhibiting activity (EC $_{50}$: 3.2 pM vs 4.9 pM). Likewise, their cytotoxic effects following electroporation were comparable, with EC $_{50}$ values of 0.7 nM for nGel and 0.8 nM for rGel (Fig.1).

These results demonstrate an efficient, scalable method for producing high purity rGel with functional properties equivalent to the native protein. It also

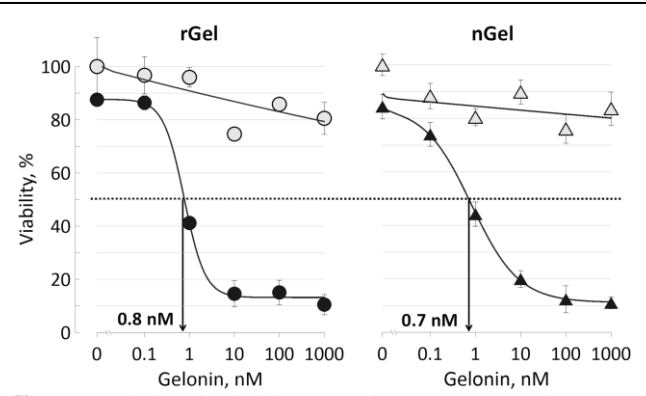


Figure 1: rGel and nGel show similar cytotoxicity after electroporation in CT26 cells (EC $_{50}$: 0.8 and 0.7 nM). Filled symbols: $8\times100~\mu s$, 1.1~kV/cm; open symbols: sham.

provides a flexible platform for fluorescent labeling to track protein delivery and intracellular trafficking. Moreover, this system supports the design of engineered rGel variants, such as those with reduced size or altered surface charge, to improve tissue penetration and therapeutic performance

- [1] Pizzo E., *et al.* A new age for biomedical applications of ribosome inactivating proteins (RIPs): from bioconjugate to nanoconstructs. *J Biomed Sci*, 23, :54, 2016.
- [2] Pakhomova O. N., *et al.* Potentiation of gelonin cytotoxicity by pulsed electric fields. *Int J Mol Sci*, 26:458, 2025.

Assessing the safety of pulsed field ablation in the presence of implantable medical devices

Bakhtawar Bibi, Bor Kos, Damijan Miklavcic; Faculty of Electrical Engineering, University of Ljubljana, Trzaska 25, SI-1000 Ljubljana, SLOVENIA

INTRODUCTION

Catheter ablation is a well-established treatment for atrial fibrillation (AF). According to Chun et al. [1], Pulsed field ablation (PFA) induces irreversible electroporation by applying high-intensity, shortduration electric fields, which disrupt myocardial cell membranes and ultimately cause cell death. A potential issue is that PFA involves the delivery of very high voltage pulses up to 2000 Volts which raises the possibility of electrical arcing and increased heating when performed near metallic components of intracardiac devices [2]. The aim of this study was to develop a numerical model to investigate the interaction between pulsed field ablation and atrial appendage occlusion devices, with particular focus on the influence of device with respect to catheter spacing on electric field distribution and potential safety risks due to excess heating.

MATERIALS AND GEOMETRY

For this study, a numerical model was developed using the finite element method in COMSOL. The simulation geometry consisted of a rectangular tissue block measuring $100 \text{ mm} \times 100 \text{ mm} \times 60 \text{ mm}$. Within this domain, a circular disk representing an implantable device specified as a schematic representation of an atrial appendage occlusion device, with the material properties of nitinol was centrally positioned. A bipolar ablation catheter, modeled with platinum material properties, was placed vertically relative to the disk. The catheter spacing, defined as the distance between the ablation catheter tip and the occlusion device surface was systematically varied, with distances ranging from 1 mm to 10 mm along the z-axis and from 1 mm to 20 mm along the x-axis. Simulations were performed to evaluate the electric field distribution and associate temperature changes under varying conditions. The applied voltage was set to 1800 V, with a duty factor of 0.01 and a total duration of 0.2 s. A physics-controlled mesh with a normal element size was used, providing refined resolution of the electric field gradients in the regions surrounding both the device and the catheter. A time dependent simulation was carried out to calculate the temperature rise in the vicinity of the catheter, and the extent of irreversible ablation was quantified by measuring the tissue volume that exceeded 100 °C, expressed in cubic millimeters (mm³).

RESULTS AND FIGURES

The simulation results showed that PFA generated localized heating and strong electric fields near the catheter electrodes, with temperatures reaching up to $100\,^{\circ}$ C. Fig 1 (a) illustrates that the region exceeding

the electroporation threshold (≥550 V/cm) extends broadly around the catheter tip and across the device surface, the tissue volume with $|E| > 550 \text{ V} \cdot \text{cm}$ reached 1570.2 mm³. In contrast, Fig 1 (b) demonstrates that significant temperature rise occurs only in the immediate vicinity of the catheter and device, with localized hot spots approaching and exceeding 90 °C. The surface map of tissue volume above 70 °C further emphasizes this trend, showing the substantial thermal effects are confined to cases where the catheter is positioned very close to the device like 1 mm or 2 mm in both directions. At larger separations, the ablation effect is dominated by non-thermal electroporation with minimal heating. These results suggest that while PFA near a device can reliably achieve electroporation, thermal side effects become significant only when the catheter is in a very close proximity to the metallic surface.

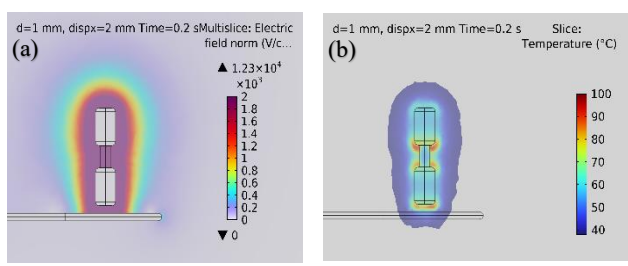


Figure 1: Electric field and temperature distribution.

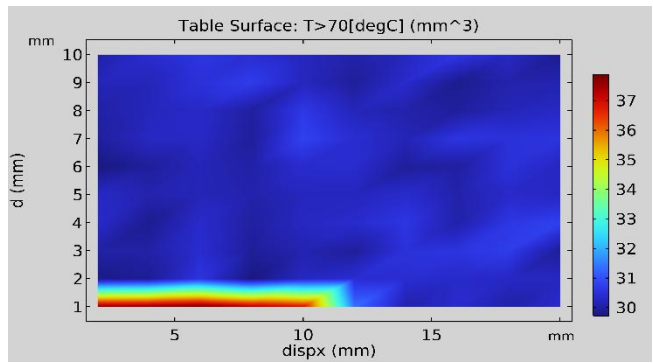


Figure 2: Simulated Tissue Volume Exceeding 70 °C.

- [1] Chun. K. -R. J., *et al.* State of the art pulsed field ablation for cardiac arrhythmias: ongoing evolution and future perspective. *EP Europace*, 26:euae. 134, 2024.
- [2] Campos-Villarreal D., et al. Visible arcing observed with pulsed field ablation applications delivered near a left atrial appendage Occlusion Device. Heart Rhythm, 2025.

Strategies to mitigate bipolar cancellation in nano-electrochemotherapy for melanoma

Egle Mickeviciute-Zinkuviene^{1,2}, Vitalij Novickij^{1,2}; ¹State Research Institute Centre for Innovative Medicine, Department of Immunology and Bioelectrochemistry, Vilnius, LITHUANIA; ²Vilnius Gediminas Technical University, Faculty of Electronics, Vilnius, LITHUANIA

INTRODUCTION

Bipolar cancellation—a phenomenon in which the effect of a positive electric pulse (\uparrow) is neutralized by a subsequent negative pulse (\downarrow) —poses a significant challenge in the efficacy of electrochemotherapy.[1] This effect can impair the permeabilization of cell membranes, leading to suboptimal delivery of drugs (bleomycin) and reduced treatment outcomes, particularly in the context electrochemotherapy. Our pilot studies confirmed that bipolar cancellation compromises treatment effectiveness not only in vitro but also in animal models. [2] To overcome this limitation, we protocolsasymmetric electric pulse modifying pulse duration and amplitude—to disrupt cancellation effects and enhance electrochemotherapy. We evaluated their potential to improve bleomycin electrochemotherapy efficacy using the B16-F10 cell line.

METHODS

To assess membrane permeabilization efficiency, B16-F10 melanoma cells were treated with the Yo-Pro®-1 dye and exposed to nanosecond pulsed electric fields. To address bipolar cancellation, we introduced asymmetry into bipolar pulses by keeping the positive-phase (↑) pulse at 12.5 kV/cm and reducing the amplitude of the negative-phase (\downarrow) pulse and increased time (ns). Membrane permeabilization was quantified by Yo-Pro® uptake via flow cytometry, while cell viability following electroporation with bleomycin was assessed using PrestoBlue after a 48-hour incubation.

RESULTS AND FIGURES

We observed the effects of pulse asymmetry in duration and amplitude using 12.5 kV/cm \times 100 pulses. The symmetric $\uparrow 200$ ns + $\downarrow 200$ ns pulse resulted in less than 20% permeabilization, likely due to strong bipolar cancellation, while ↑200ns + ↓600ns pulse induced high permeabilization across nearly all tested amplitudes. The ↑200ns + ↓400ns pulse effectively reduced bipolar cancellation, especially at amplitudes of 10-15~kV/cm, with 12.5~kV/cmachieving cytotoxicity comparable to ESOPE-standard 1). Further we (Fig. compared permeabilization results of the 12.5 kV/cm protocol and the respective efficacy of ECT with bleomycin Cell viability assays showed that the cancellation phenomenon significantly affects the efficacy of ECT, thus only the asymmetric ↑200+↓600 ns pulse protocol caused effective ECT. In contrast, bipolar pulses without asymmetry did not cause any significant cell death. In conclucions, asymmetric nanosecond pulses significantly

electroporation efficacy compared to symmetric pulses, due to reduction of the bipolar cancellation.

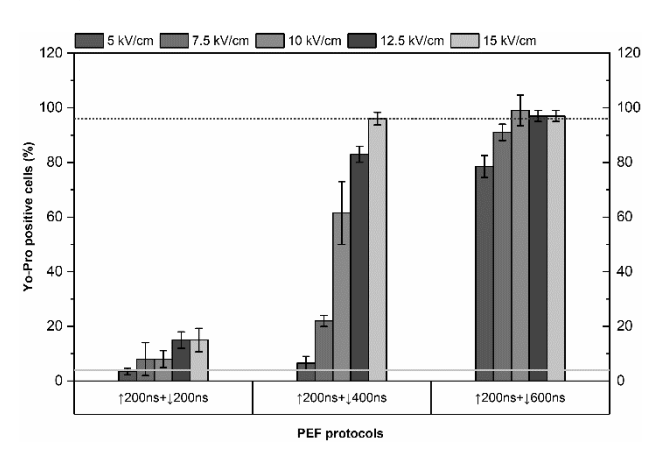


Figure 1: Yo-Pro uptake caused by permeabilization: $5-15 \, kV/cm$; $\uparrow 200 \, ns + \downarrow 200/400/600 \, ns$; 100 pulses. Dotted line shows PCTRL, straight line shows NCTRL.

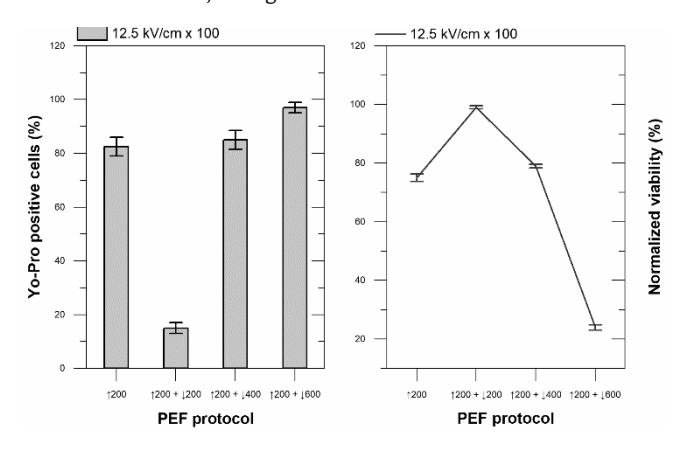


Figure 2: On the left cell permeability assessed with Yo-Pro: at 12.5 kV/cm×100 pulses (\uparrow 200 ns, \uparrow 200+ \downarrow 200/400/600ns); in comparison to right cell viability assessed with PrestoBlue: at 12.5 kV/cm × 100 pulses (\uparrow 200 ns + \downarrow 400 ns).

- [1] Pakhomov A. G., *et al.* Interference targeting of bipolar nanosecond electric pulses for spatially focused electroporation, electrostimulation, and tissue ablation. *Bioelectrochemistry*, 141:107876, 2021.
- [2] Mickevičiūtė E., *et al.* The effects of bipolar cancellation phenomenon on nano-electrochemotherapy of melanoma tumors: in vitro and in vivo pilot. *Int J Mol Sci.*, 25, 2024.

High-power pulsed electromagnetic fields combination with calcium chloride or bleomycin for 4T1 breast cancer treatment: an *in vivo* study

Augustinas Želvys^{1,2}, Vitalij Novickij^{1,2}; ¹State Research Institute Centre for Innovative Medicine, Department of Immunology and Bioelectrochemistry, Vilnius, LITHUANIA; ²Vilnius Gediminas Technical University, Faculty of Electronics, Vilnius, LITHUANIA

INTRODUCTION

Electroporation (EP) is a phenomenon of reversible or irreversible permeabilization of biological cells, which is triggered by cell polarization in pulsed electric fields (PEF). This leads to the formation of aqueous pores in the phospholipid bilayer (electroporation, EP), where normally impermeable substances, such as chemotherapeutic drugs, can freely move through the formed nanopores according to their concentration gradient. Usage of chemotherapeutics with EP is called electrochemotherapy (ECT). ECT is undoubtedly one of the most effective cancer treatments, however, the methodology requires direct contact with tissue [1], [2]. Application of high pulsed electromagnetic fields (HI-PEMF) in this context could solve this limitation and the problems associated with field homogeneity, muscle contractions and oxidation. Similar to EP, the temporary physical loss of membrane integrity after HI-PEMF application can be detected conventional fluorescent markers such as PI or YO-PRO-1[3].

This is the first *in vivo* study where HI-PEMFs are used in combination with calcium ions or bleomycin for cancer treatment.

METHODS

The BALB/c linear *Mus musculus* (mice) were used in this study. The tumors were induced in 6-8 week-old mice by subcutaneously injecting 4T1 breast cancer cells. When the tumors reached ~100 mm³, mice were randomly grouped: CTRL (untreated tumor-bearing control), HI-PEMF only (treated only with HI-PEMF), HI-PEMF + CaCl₂ (treated with both of CaCl₂ solution (250 mM calcium chloride in sterile saline buffer) (i.t.) and HI-PEMF) and HI-PEMF + BLM (Treated with both of bleomycin drug (1500 IU in 50 μ L of sterile saline buffer) (i.t.) and HI-PEMF). The mice were kept till the end of the experiment (or when primary tumors had reached ~1000 mm³ volume) at which point they were euthanized. For HI-PEMF a high-power pulsed generator was used generating oscillating sine waveform [4]. The 3.5 T \times 1000 (20 Hz) pulsing protocol was employed in the study. Mice survival and tumor dynamics were assessed during the study.

RESULTS

We observed a significant change in survival between treatment groups (Fig. 1). Mice that have been treated only with HI-PEMF survived significantly longer than the untreated control. The longest survival are in the groups where HI-PEMFs were combined with either bleomycin or CaCl $_2$ solution. In HI-PEMF + CaCl $_2$ treatment group few mice healed entirely. Assessing tumor volume dynamics revealed that only

in the HI-PEMF + $CaCl_2$ treatment group tumors where completely gone in surviving mice, after 22-24 days after the treatment (Fig.2).

In conclusion HI-PEMF combination with the $CaCl_2$ or chemotherapeutics can be successfully used for further cancer treatment studies *in vivo*.

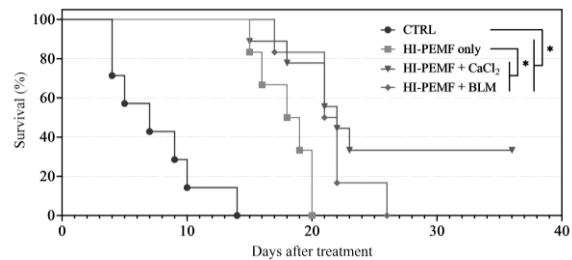


Figure 1: Kaplan–Meier survival curves of mice with 4T1 breast cancer tumors treated with or without combination of HI-PEMF and $CaCl_2$ or Bleomycin injections. The asterisk (*) highlights statistically significant differences (Mantel–Cox test; * p < 0.05).

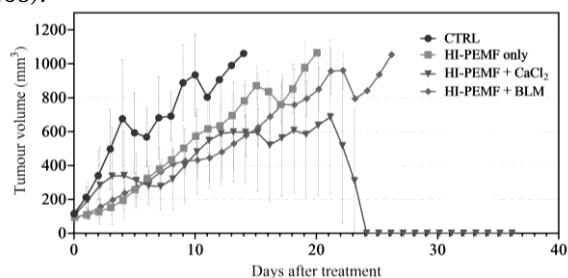


Figure 2: Volumetric tumor growth changes of mice with 4T1 breast cancer tumors after the treatment with or without combination of HI-PEMF and CaCl $_2$ or bleomycin injections. Error bars denote group's min and max volumes.

Acknowledgements: The research was funded by the Research Council of Lithuania Grant Nr. S-MIP-23-124.

- [1] Čorović S., *et al.* Analytical and numerical quantification and comparison of the local electric field in the tissue for different electrode configurations. *Biomed Eng Online*, 6: 37, 2007.
- [2] Yarmush M. L., *et al.* Electroporation-based technologies for medicine: principles, applications, and challenges. *Annu Rev Biomed Eng*, 16: 295–320, 2014.
- [3] Novickij V., *et al.* High-pulsed electromagnetic field generator for contactless permeabilization of cells In vitro. *IEEE Trans Magn*, 56:pp. 1-6,2020.
- [4] Staigvila G., *et al.* Fast ignitron-based magnetic field pulser for biological applications. *IEEE Trans Magn*, 55:1-5, 2019.

Characterization of electrochemotherapy induced cell death pathways in vitro

Lara Snoj^{1,2}, Gregor Sersa^{1,3}, Amar Balihodzic⁴, Michael Dengler⁴, Maja Cemazar^{1,5}, Bostjan Markelc^{1,5}; ¹Department of Experimental Oncology, Institute of Oncology Ljubljana, SLOVENIA; ²Faculty of Medicine, University of Ljubljana, SLOVENIA; ³Faculty of Health Sciences, University of Ljubljana, SLOVENIA; ⁴Department of Internal Medicine, Division of Oncology, Medical University of Graz, AUSTRIA; ⁵Faculty of Health Sciences, University of Primorska, Izola, SLOVENIA; ⁶Biotechnical Faculty, University of Ljubljana, SLOVENIA

INTRODUCTION

Electrochemotherapy (ECT) is a local ablative therapy that uses electric pulses to transiently increase cell membrane permeability, therefore enhancing the uptake of chemotherapeutic agents such as Bleomycin (BLM), Oxaliplatin (OXA) and Cisplatin (CDDP) into the cells, potentiating their cytotoxic activity. In addition to its direct cytotoxic effects, ECT can also promote anti-tumor activity by inducing immunogenic cell death (ICD), which can elicit an adaptive immune response against neo-antigens released from dying tumor cells, effectively converting them into an in situ cancer vaccine [1].

BACKGROUND

The immunogenic characteristics of ICD are mainly mediated by the release of molecular signals, called damage-associated molecular patterns (DAMPs). Two types of DAMPs have been described: constitutive DAMPs (cDAMPs), which are normally present inside healthy cells and released upon plasma membrane rupture, and inducible DAMPs (iDAMPs), which are synthesized in response to stress or cell death. For cell death to be considered immunogenic, both types of DAMPs have to be released in a coordinated manner to successfully activate adaptive immunity [2]. However, DAMPs are only released in certain types of cell death. Therefore, the aim of our study is to determine which death pathways induced electrochemotherapy in vitro.

METHODS

We have generated B16F10 and CT26 cell lines, lacking genes for apoptosis (Bax and Bak), necroptosis (RIPK3 and MLKL) and pyroptosis (GSDME and GSDMD), using the CRISPR-Cas9 system. For the nucleofection we used SF Cell Line 4D-Nucleofector X kit S from Lonza. These cell lines were used to investigate the contribution of specific cell death pathways to ICD after ECT with BLM, OXA and CDDP. For ECT, cells were trypsinized, centrifuged and resuspended in cell medium without FBS. Then 1x10^6 cells in drug-containing medium were placed between stainless steel electrodes (2 mm gap between them) and electroporated with 8 square-wave pulses (1300 V/cm, 100 µs duration at frequency of 1 Hz). The cell mixture was then transferred into 24-well ultra-low

attachment plate and 5 min after pulse delivery, 1 ml of cell culture medium was added. Cells were seeded in 96-well plates in 100 uL of cell culture medium and their survival was measured at 24 and 72 h after ECT using Presto Blue.

RESULTS

Elimination of apoptotic effectors (Bax/Bak) or pyroptotic effectors (GSDME/D) in separate cell lines provided only small protection, indicating that loss of these pathways alone does not fully prevent cell death after ECT.

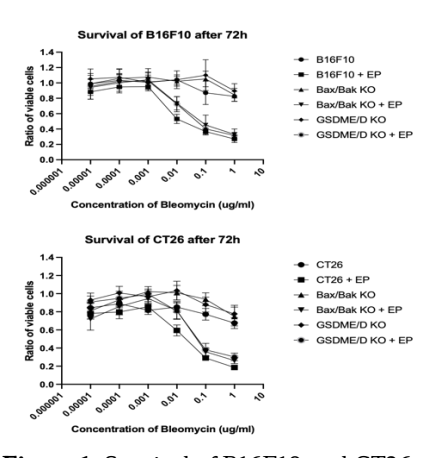


Figure 1: Survival of B16F10 and CT26 cell lines (normal and KO) after ECT with different concentrations of BLM.

CONCLUSIONS

Our findings indicate that apoptosis and pyroptosis are not the main pathways of cell death induced by ECT. Further investigation is needed to identify the predominant mechanisms responsible for its cytotoxic and immunogenic effects.

- [1] Kesar U., *et al.* Effects of electrochemotherapy on immunologically important modifications in tumor cells. *Vaccines*, 11: 925, 2023.
- [2] Kepp O., *et al.* Molecular determinants of immunogenic cell death elicited by anticancer chemotherapy. *Cancer Metastasis Rev*, 30: 61-69, 2011.

Calcium electrochemotherapy using ultra-fast nanosecond electric pulses and their effects on mitochondria transmembrane potential and oxidation

Paulina Malakauskaite^{1,2}, Vytautas Kaseta³, Vitalij Novickij^{1,2}; ¹State Research Institute Centre for Innovative Medicine, Department of Immunology and Bioelectrochemistry, Vilnius, LITHUANIA; ²Vilnius Gediminas Technical University, Faculty of Electronics, Vilnius, LITHUANIA; ³State Research Institute Centre for Innovative Medicine, Department of Stem Cell Biology, Vilnius, LITHUANIA

INTRODUCTION

Electroporation refers to the phenomenon wherein the application of high, short-duration pulsed electric fields (PEF) to biological cells induces a transient increase in plasma membrane permeability [1]. The pulse duration of nanosecond PEF (nsPEF) is significantly shorter than the time constant of biological cell membrane and can penetrate into the interior of the cell and organelles inducing various biological effects [2]. Thus, nsPEF alter mitochondrial function by permeabilizing its membrane.

Mitochondria must maintain the electric potential across the inner membrane and a loss of the proton gradient often leads to the disruption of the potential membrane mitochondrial and couples with the ROS-induced oxidative stress [3]. Both of these signalling systems profoundly influences the rate of ATP synthesis [4], which is also linked to calcium overload [5]. Mitochondrial calcium overload also work complementarily with ROS overproduction and dependent on the mitochondrial membrane potential [6]. All of these processes ultimately causes cell death involving apoptosis or necrosis. Therefore, stimulation of apoptosis through a mitochondrialmediated pathway with nsPEF could enhance current electrochemotherapy protocols.

METHODS

Pulses were generated using a custom-built high-frequency (up to 6.6 MHz) square-wave generator ($\leq 3~\rm kV$). The voltage varied in 50 V - 1.6 kV range, corresponding to a 0.5–16 kV/cm electric field in the cuvette. We applied 50 ns or 300 ns monophasic pulses (100 pulses/burst, 100 ns delay) and a microsecond reference protocol (1.2 kV/cm \times 100 $\mu s \times$ 8, 1 Hz). CHO-K1-Luc cells were used as a model. Permeabilization was detected with Yo-Pro-1, MMP disruption with TMRM, ROS with MitoSOX Red, ATP depletion via D-luciferin oxidation, and viability via PrestoBlue. For CaECT, CaCl $_2$ (5 mM) was added in low-conductivity HEPES buffer (10 mM HEPES, sucrose, 1 mM Mg $^{2+}$).

RESULTS

High permeabilization (>75 %) was achieved with pulsed electric field exceeding 6 kV/cm for 50 ns pulses and 4 kV/cm for 300 ns (n = 100), respectively. PEF amplitude was limited to 6–12 kV/cm protocols to

ensure overlapping points in terms of permeabilization efficacy for both 50 ns and 300 ns protocols.

300 ns pulses caused a greater MMP reduction than 50 ns pulses, indicating that high permeabilization is required to trigger significant depolarization of mitochondria within the studied parametric range.. Both nsPEF (>50 ns) and microsecond pulses affected MMP only above the outer membrane electroporation threshold.

In the context of ROS, 300 ns pulses trigger detectable oxidation of mitochondria even without added calcium. When calcium is added in both cases (50 ns and 300 ns) the oxidation of mitochondria increases up to $2000\,\%$.

The highest ATP depletion following CaECT is triggered when the highest PEF amplitude was involved in the study. All the protocols involved in the study resulted in detectable ATP depletion.

A viability assay showed that 300 ns pulses at >6 kV/cm caused partly irreversible electroporation and cell death in all CaECT protocols, while 50 ns pulses (6-12 kV/cm) induced reversible electroporation. For 50 ns pulses, 10-12 kV/cm enabled sufficient calcium electrotransfer for effective CaECT in vitro. Compared to the ESOPE protocol, nanosecond pulses achieved high electrochemotherapy efficiency and ultra-high frequency bursts lowered permeabilization thresholds, enabling 50 ns pulses at 10 kV/cm for successful CaECT *in vitro*.

- [1] Kotnik T., *et al.* Membrane electroporation and electropermeabilization: mechanisms and models. *Annu Rev Biophys*, 48:63-91, 2019.
- [2] Ruiz-Fernández A. R., et al. Nanosecond pulsed electric field (nsPEF): opening the biotechnological Pandora's box. Int J Mol Sci, 23:6158, 2022.
- [3] Fahimi P., *et al.* Electrical homeostasis of the inner mitochondrial membrane potential. *Physical biology*, 22, 2025.
- [4] Nicholls D. G. Mitochondrial membrane potential and aging. *Aging Cell*, 3:35-40, 2004.
- [5] Ohnishi N., *et al.* Variations of intracellular Ca2+ mobilization initiated by nanosecond and microsecond electrical pulses in HeLa cells. *IEEE Trans Biomed Eng*, 66:2259-2268, 2019.
- [6] Tarasov A. I., *et al.* Regulation of ATP production by mitochondrial Ca(2+). *Cell Calcium*, 52:28-35, 2012.

Electrochemotherapy for spontaneous tumors in cats: establishing VetINSPECT platform

Tanya Birk¹, Urša Lampreht Tratar¹, Maja Čemažar^{2, 4}, Gregor Serša^{2, 3}, Nataša Tozon¹; ¹University of Ljubljana, Veterinary Faculty, SLOVENIA; ²Institute of Oncology Ljubljana, SLOVENIA; ³University of Ljubljana, Faculty of Health Sciences, SLOVENIA; ⁴University of Primorska, Faculty of Health Sciences, Izola, SLOVENIA

INTRODUCTION

Electrochemotherapy (ECT) has proven to be an effective local treatment modality in veterinary medicine for managing various types of neoplasia in dogs and cats, achieving an approximate success rate of 80%, depending on the tumor type. In Slovenia, ECT has been performed for about 30 years, during which more than 200 animals have been treated with ECT as a standalone therapy [1]. To enable better monitoring and comparison of treatment outcomes, we envisioned the establishment of a database like that used in human oncology (INSPECT) – VetINSPECT [2].

METHODS

ECT was performed using an intravenous application of bleomycin. The dose was 15,000 IU/m² of body surface area (BSA). Bleomycin (Bleomycin medac, 15,000 IU = 10 mg) was stored refrigerated and reconstituted with 3.3 mL saline to achieve a concentration of 4,500 IU/mL (3 mg/mL). Adter intravenous aaplication pulses were applied after 8 minutes and completed within 28 minutes to ensure optimal intratumoral drug concentration. Electroporation of the tumors was performed using an electric pulse generator (Cliniporator, IGEA S.p.A., Carpi, Italy). Appropriate needle or plate electrodes were selected based on tumor size and location to ensure optimal electric field distribution [3].

RESULTS

A total of 94 cats were included in the study, with a median age of 11.4 years (range 0-20.2) and a median body weight of 4.7 kg (range 2.0–11.4). The mean body surface area was 0.3 m². The cohort consisted of 51 males (54%) and 43 females (46%). Previous surgery had been performed in 12% of cases, while all tumors were primary. The most common diagnosis was squamous cell carcinoma (SCC, 65.7%), followed by mast cell tumor (MCT, 11.7%), and other tumor types including carcinoma (4.3%), Bowenoid in (3.2%),carcinoma (BISC) (4.3%),sarcoma fibrosarcoma (2.1%), peripheral nerve sheath tumor (FSA/PNST) (2.1%), and several single cases (1.1% each) of basal cell carcinoma (BCC), soft tissue sarcoma (STS), leiomyosarcoma, melanoma, myeloma, and myxosarcoma [2] (Fig. 1).

A total of 138 nodules were treated across 94 cats, with a median size of 10 mm (range 1–65 mm; mean 12 mm). The most common tumor location was the nose (39.9%), followed by the ear pinna (21.7%), legs

including thigh, paw, and elbow (13.8%), eyes (5.1%), and lips (4.3%). Less frequent sites included the dorsal thoracic region (3.6%), back (2.9%), head (2.2%), neck (2.2%), mouth (1.4%), tail (0.7%), chin (0.7%), mammary gland (0.7%), and unknown locations (0.7%) [2].

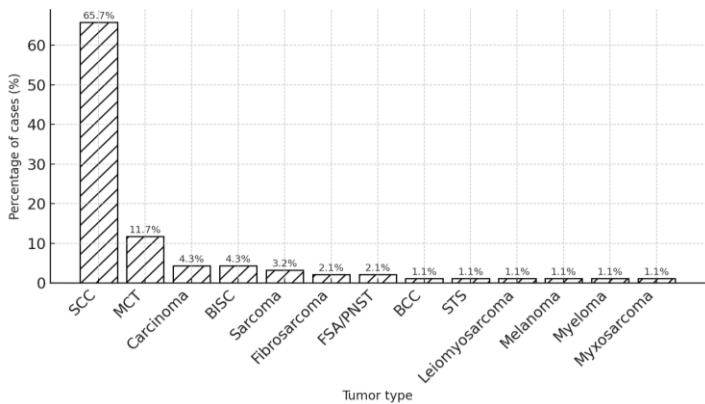


Figure 1: Tumor type distribution among included cats (n = 94).

The treatment was the most successful in case of carcinomas, then MCT, SCC and sarcomas, where the complete response was achieved in 95%, 90%, 74% and 33%, respectively (p=0.0013).

CONCLUSIONS

The VetINSPECT platform proved to be a suitable and reliable tool for collecting and analyzing clinically relevant data. By standardizing data acquisition, it enables meaningful comparison of treatment outcomes in veterinary oncology.

- [1] Tozon N., *et al.* Operating procedures of the electrochemotherapy for treatment of tumor in dogs and cats. *JOVE*, 116:e54760, 2016.
- [2] Tozon N., et al. Predstavitev VetINSPECT baze in preliminarnih rezultatov," III. Slov. kongres elektroporacije, program in knjiga povzetkov, Ljubljana, Slovenia, 16, 2025. [Online].
- [3] Tozon N., *et al.* Electrochemotherapy with intravenous bleomycin injection: an observational study in superficial squamous cell carcinoma in cats. *J Feline Med Surg*, 16: 291-299, 2013.

Induction of the bystander effect in 3D cell cultures after electroporation-based treatments *in vitro*

Augustinas Šarkinas, Neringa Barauskaitė-Šarkinienė, Paulius Ruzgys, Saulius Šatkauskas; Laboratory of Cell and Tissue Biotechnology, Research Institute of Natural and Technological Sciences, Vytautas Magnus University, Universiteto str. 10, Akademija, Kaunas district LT-53361, LITHUANIA

INTRODUCTION

Despite significant progress in oncology, the limitations of conventional cancer treatments necessitate the exploration of novel therapeutic strategies. Electric field-based therapies, including electrochemotherapy (ECT) and irreversible electroporation (IRE), have emerged as potent methods for localized tumor ablation. These techniques utilize the principle of electroporation, where applied electric pulses create transient or permanent pores in the cell membrane, either facilitating the entry of anticancer drugs or directly causing cell death through loss of homeostasis.

A critical gap in our understanding of these therapies is the extent of their non-local effects. This line of inquiry parallels the well-documented "bystander effect" in radiotherapy, where untreated cells are affected by signals from their irradiated neighbouring cells [1]. While research into an analogous effect for electroporation is recent, preliminary evidence has confirmed its existence *in vitro* for specific cell lines [2,3].

This study aims to characterize the bystander effect induced by electric field-based therapies in three-dimensional *in vitro* models. Utilizing both non-cancer CHO and cancer 4T1 cell lines, we investigated how signals from treated cells impact the viability of untreated 3D cells.

MATERIALS AND METHODS

The experiments were conducted using Chinese Hamster Ovary (CHO) and mouse breast cancer (4T1) cell lines. The electrotransfer of CaCl $_2$ and the anticancer drug bleomycin (BLM) into cell suspension was achieved using a single electrical pulse of 1400 V/cm with a duration of 100 μs . For irreversible electroporation, a single 100 μs pulse with an amplitude of 2800 V/cm was applied.

To initiate spheroid (3D) cell cultures, the bottom of 96-well plates was coated with 2% agarose to create concave, "U"-shaped microwells. A suspension of 15,000 cells was added to each well, and the volume was adjusted to a final total of 200 μL with additional culture medium.

To generate conditioned (bystander) medium, cell suspension were subjected to either BLM electrotransfer, calcium electroporation, or irreversible electroporation. The conditioned medium was collected after 24 and 48-hour incubation periods for subsequent use in 3D bystander effect studies.

Following the incubation, the conditioned medium was harvested from the treated cell in a form of

suspension, centrifuged twice to eliminate cellular debris, and then transferred to untreated 5-day-old 3D spheroid cultures. The spheroids were imaged using microscope every two days for a total of 14 days. Their cross-sectional area was measured to calculate the volume, which served as a metric for growth assessment.

RESULTS AND DISCUSSION

This study reveals that the bystander effect induced by electric field-based therapies has a dual nature; it can either stimulate or inhibit the viability of indirectly exposed cells depending on the applied electric field parameters. Furthermore, our investigation assessed the impact of these anticancer therapies on 3D cell cultures. A key finding is that the bystander effect originating from 2D cell cultures significantly influences the viability of 3D structures. To our knowledge, this is the first comprehensive study to investigate the bystander effect of electric field-based anticancer therapies in three-dimensional *in vitro* cell cultures.

The bystander effect from 2D cells treated with BLM electrotransfer negatively impacted the viability of both CHO and 4T1 spheroids. In contrast, both calcium electroporation and irreversible electroporation induced a positive bystander effect when the conditioned medium was collected after 24 hours, but a negative effect when collected after 48 hours.

CONCLUSIONS

After exposure to bleomycin electrotransfer, the bystander effect induced by cell monolayer affects the viability of spheroid cells in both CHO and 4T1 cell lines. After both calcium and irreversible electroporation, a positive bystander effect was observed when the bystander medium was transferred at 24 hours, whereas a negative bystander effect was observed when the medium was transferred at 48 hours.

- [1] Jalal N., et al. Radiation induced bystander effect and DNA damage. J Cancer Res Ther, 10:819-833, 2014.
- [2] Ruzgys P., et al. The evidence of the bystander effect after bleomycin electrotransfer and irreversible electroporation. *Molecules*, 26:6001, 2021.
- [3] Barauskaitė-Šarkinienė N., *et al.* Investigation of the bystander effect on cell viability after application of combined electroporation-based methods. *Int J Mol Sci*, 26:2297, 2025.

The investigation of synergistic effects of nivolumab and cisplatin electrotransfer *in vivo*

Diana Šiurnaitė¹, Greta Chlebopaševienė², Paulius Ruzgys¹, Saulius Šatkauskas¹; ¹Biophysical Research Group, Vytautas Magnus University, Universiteto st. 10, LT-53361 Akademija, Kaunas District, LITHUANIA; ²Institute of Oncology, Lithuanian University of Health Sciences, LITHUANIA

INTRODUCTION

Electroporation is a technique that uses electrical pulses to increase cell membrane permeability, facilitating drug delivery or directly killing cells. Checkpoint therapy is a type of immunotherapy that targets proteins cancer cells use to hide from the immune system, freeing up the body's natural defenses to fight the tumor [1]. We investigated whether combining these modalities offers superior tumor control compared to individual treatments. This study explores the combined effects of cisplatin chemotherapy, electroporation and checkpoint therapy in treating tumors.

MATERIALS AND METHODS

Cultivation of the Cells

Experiments were performed using breast cancer cell line 4T1 (ATCC). Cells were cultured in RPMI media (Sigma-Aldrich, Saint Louis, MO, USA), supplemented with 1% penicillin-streptomycin (Sigma-Aldrich) and 10% fetal bovine serum (Sigma-Aldrich).

Experimental Scheme

Eight to twelve-week-old female BALB/c mice were used in the experiments. The tumor induction was performed by administering one 100 μL subcutaneous injection (s.c.) that contained 4T1 cells (20 mln/ml). One tumor was induced on a single mouse. The tumors were allowed to establish and grow until they reached $\sim\!150{-}500~mm^3$. Depending on the tumor growth rate, the experiments were performed 10 days after the injection.

Mice were divided into nine groups by total tumor volume to create balanced groups. (1) Untreated tumor-bearing mice (CTRL) (n=8), (2) mice treated with cisplatin (Cis) (n=8), (3) treated with cisplatin and electroporation (Cis + EP) (n=8), (4) mice treated with only electroporation

(EP) (n=8), (5) mice treated only with checkpoint therapy (Ch.P) (n=8), (6) mice treated with checkpoint therapy and electroporation (Ch.P + EP) (n=4),(7) mice treated with checkpoint therapy, electroporation and cisplatin (Ch.P + EP + Cis)(n=8),(8) mice treated with only irreversible electroporation(IRE)(n=8), (9) mice treated with irreversible electroporation and checkpoint therapy (IRE + Ch.P) (n=8)

Before the experimental procedures (on day -1), the area where tumors were present was shaved, and the remaining hair was removed with depilatory cream. Before treatment, an anesthetic solution was made of a mixture of ketamine (80 mg/kg), xylazine (7.5 mg/kg) and diluted with isotonic saline (0.9% NaCl). The anesthetics were administered intraperitoneally (I.P). *Electroporation*

Electroporation was performed using a BTX T820 electroporator (Harvard Apparatus, San Diego, CA, USA). Two different electroporation protocols were

used on sedated mice: (1) EP protocol (groups 3,4,6,7): 1.5 kV/cm \times 8 pulses, 99 μ s, 1 Hz. (2) IREP protocol (groups 8,9): 2.8 kV/cm \times 8 pulses, 99 μ s, 1 Hz. *Treatment with drugs*

Cisplatin 88 μL (1 mg/mL concentration) was injected as a single dose into the mouse tail vein (groups 2, 3, 7). As a checkpoint therapy drug, Nivolumab (200 μ g) was administered (I.P.) every two days for a total of four injections (groups 5, 6, 7, 9). *Evaluation of Tumor Sizes*

The tumors were measured every 2 days starting on day 1 (day of the experiment) and finishing on day 19. The volume of tumor were measured by digital caliper. Tumor volume (mm³) were calculated according the formula: $V = (\pi \ x \ l \ x \ w \ x \ h)$ /6, where l—length, h – height and w—width of the tumor. [1]

RESULTS

This experiment indicates that the most effective inhibition of tumor growth was achieved with the combination of (EP + Ch.P + Cis), where tumors showed a proliferation rate of only 2.7-fold over a 19day period. This result suggests this combined approach is the most potent strategy for controlling tumor expansion. The (EP + Cis) group also demonstrated comparable efficacy, with tumor volume increasing slightly less than threefold—a significant improvement compared to the control group, where tumor volume increased over sixfold. In contrast, the groups treated with (Ch.P + EP) and (Ch.P) showed similar but less pronounced effects, with tumor growth nearly halved relative to the control. The least effective treatments were the single therapies (EP) and (Cis), which resulted in an approximate fivefold increase in tumor size, while the (IRE) group performed slightly better at a 4.7-fold increase. Finally, the combination of (IREP + Ch.P) was more effective than using (IREP) alone but less so than using only (Ch.P), as tumor volume increased over fourfold.

CONCLUSIONS

The (EP+Ch.P+Cis) combination was the most effective strategy, confirming the superiority of multiagent therapies over single treatments in controlling tumor growth.

- [1] Hadzialjevic B., *et al.* Electrochemotherapy combined with immunotherapy a promising potential in the treatment of cancer. *Front Immunol*, 14, 2024.
- [2] Ruzgys P., *et al.* Induction of bystander and abscopal effects after electroporation-based treatments. *Cancers*, 14:3770-3770, 2022.

EBTT Proceedings 2025 FACULTY MEMBERS

Faculty members



Rafael V. Davalos Georgia Tech, USA E-mail: rafael.davalos@bme.gatech.edu



Marie-Pierre Rols IPBS-CNRS, France E-mail: rols@ipbs.fr



Julie Gehl University of Copenhagen, Department of Clinical Medicine, Denmark E-mail: kgeh@regionsjaelland.dk



Gregor Serša Institute of Oncology, Slovenia E-mail: gsersa@onko-i.si



Richard Heller College of Engineering and Morsani College of Medicine, University of South Florida, USA E-mail: rheller@usf.edu



Mounir Tarek Theoretical Physics and Chemistry Laboratory, Université de Lorraine, France E-mail: mounir.tarek@univ-lorraine.fr



Antoni Ivorra Universitat Pompeu Fabra, Spain E-mail: antoni.ivorra@upf.edu



Atul Verma McGill University, Canada E-mail: atul.verma@mcgill.ca

P. Thomas Vernier



Damijan Miklavčič University of Ljubljana, Faculty of Electrical Engineering, Slovenia E-mail: damijan.miklavcic@fe.unilj.si



Frank Reidy Research Center for Bioelectrics, Old Dominion University, **USA** E-mail:



Lluis M. Mir Université Paris-Saclay, CNRS, France E-mail: luis.mir@cnrs.fr